Mathematisches Forschungsinstitut Oberwolfach

Report No. 34/2012

DOI: 10.4171/OWR/2012/34

Discrete Differential Geometry

Organised by
Alexander I. Bobenko, Berlin
Richard Kenyon, Providence
Peter Schröder, Pasadena
Günter M. Ziegler, Berlin

July 8th– July 14th, 2012

Abstract. This is the collection of extended abstracts for the 24 lectures and the open problems session at the third Oberwolfach workshop on Discrete Differential Geometry.

Mathematics Subject Classification (2010): 52-xx, 53-xx, 57-xx.

Introduction by the Organisers

Discrete Differential Geometry is a very productive research area where graph theory, analysis, integrability, and geometry interact and contribute to the construction and understanding of discrete models for differential geometric situations and structures. It also plays a very important role in applications, to graphics and simulations of PDE.

This was the third Discrete Differential Geometry conference at Oberwohlfach. The subject has evolved significantly since its beginning a decade ago. This year's conference highlighted advances in new areas: in discrete exterior calculus and cluster algebras in geometry, as well as in some older ones: discrete uniformization, polyhedra, applications to PDE.

The workshop featured many talks around the subject of discrete exterior calculus. The main idea of discrete exterior calculus is to find the right adaptation of the classical notions of forms, exterior differentiation, Hodge decomposition, etc. to functions on cell complexes, with the goal being to do classical analysis using discrete approximations to continuous objects. The talks by Chelkak, von Deylen, Günther, Hildebrandt, Skopenkov, Stern all fit in this category. From the variety

of techniques presented we can only say that the subject is still under discussion, and that a global framework is still to be found.

Another new and exciting direction is the integrability and cluster structure of discrete geometric mappings. Here we heard talks by Doliwa, Goncharov, Suris, Tabachnikov on connections between various discrete systems and cluster algebras/varieties or other integrable structures. This area seems ripe for further exploration, in particular since we don't understand what features these models have in common, and what consequences the cluster structure may have. In particular the cluster structure allows one to introduce quantization which may yield important new avenues of research.

There were a few talks about polyhedra (by Adiprasito, Izmestiev, Schlenker) and versions of discrete uniformization (by Sechelmann, Stephenson, Sullivan). Although these are more well-studied areas the new ideas presented open new opportunities for further research.

Finally there were a few talks about discretizations of PDE: by Crane, Lessig, Schief, Schumacher, Hoffmann, Vouga. Here we include applications to graphics: mapping textures to surfaces and smoothing using conformal maps is one common theme. This area of PDE applications continues to be an important source of inspiration for theoretical advances in discrete differential geometry: our goal is to be able to model PDEs, and often finding the right discretization makes a huge difference in efficiency. Furthermore some systems have discretizations which are in some sense more natural than their continuous counterparts (in the sense that there is more mathematical structure).

The organizers are grateful to all participants for all the lectures, discussions, and conversations that combined into this very lively and successful workshop – and to everyone at Research Institute in Oberwolfach for the perfect setting.

Workshop: Discrete Differential Geometry

Table of Contents

Abstracts

Many 4-polytopes with a low-dimensional realization space

Karim A. Adiprasito
(joint work with Günter M. Ziegler)

We report on recent progress [1] on two classical problems concerning the space of geometric realizations of a given polytope. The first problem seems to originate with Perles. A d-polytope $P \in \mathbb{R}^d$ is *projectively unique* if every polytope P' in $\mathbb{R}^d$ combinatorially equivalent to P is related to P via a projective transformation.

Problem I (Perles & Shephard '74 [8], Kalai '97 [5])**.** *Is it true that, for fixed d, the number of distinct combinatorial types of projectively unique d-polytopes is finite?*

It was generally conjectured that the answer to this problem is positive, even though no substantial progress was made since 1976 [7]. It is easy to see that a 2-polytope is projectively unique if and only if it has 3 or 4 vertices. The case of 3-polytopes is more demanding. Classical approaches highlight the close connection of Problem I to the dimension of the *realization space* $\mathcal{RS}(P)$ (cf. [12]) of a polytope P.

Theorem 1 (Legendre–Steinitz Formula [11, Sec. 69, p. 349])**.** *The realization space of a 3-polytope P is of dimension $f_1(P) + 6$.*

From this, we can see that a 3-polytope can be projectively unique only if $f_1(P) + 6 \leq \dim \mathrm{PGL}(\mathbb{R}^4) = 15$. A more careful analysis reveals that this is in fact a complete characterization: A 3-polytope is projectively unique if and only if it has at most 9 edges [3, Sec. 4.8, pr. 30].

This argument motivates the study of the dimension of the realization space of a polytope as a separate problem, which goes back to research of Legendre. He was the first to give the correct formula (Theorem 1) for the dimension of the realization space of 3-polytopes, cf. [6, Note VIII, p. 309], the first proof for which was later supplied by Steinitz [11, Sec. 69].

Let the *size* of a polytope be given by the combined number of its vertices and facets. We study Legendre's problem in the following form:

Problem II (Legendre–Steinitz; cf. Ziegler 2011 [12])**.** *How does, for d-dimensional polytopes, the dimension of the realization space grow with the size of the polytopes?*

Main Idea and Results. Our approach to these problems is given by the observation that the 8-th vertex of a realization of the 3-cube is determined by the remaining 7 vertices. This idea gives rise to a construction technique for cubical complexes as follows: We give a sequence of cubical 3-complexes $\mathcal{T}_n,\ n \in \mathbb{N}$, called *transmitters*, such that for every construction step $\mathcal{T}_{n-1} \to \mathcal{T}_n$, $\mathcal{T}_n$ is obtained from $\mathcal{T}_{n-1}$ by attaching a (combinatorial) 3-cube W to $\mathcal{T}_{n-1}$ such that $\mathcal{T}_{n-1} \cap W$ has 7 vertices. Since the geometric realization of the attached cube is determined by

the information in $\mathcal{T}_{n-1}$, the geometric realization of $\mathcal{T}_n$ is determined by the realization of $\mathcal{T}_{n-1}$, and in particular, the geometric realization of $\mathcal{T}_n$ is determined by the realization of $\mathcal{T}_0$.

With this technique, we are able to complete the answer to Problem II.

Theorem I (Transmitter polytopes, A.-Ziegler [1])**.** *There is an infinite family* $(\mathrm{TRP}_4[n])$, $n \in \mathbb{N}$ *of combinatorially distinct* 4*-dimensional polytopes on* $24 + n$ *vertices, such that for all* n, $\dim \mathcal{RS}(\mathrm{TRP}_4[n])$ *is bounded above by* 96*.*

As an immediate corollary, we obtain:

Corollary 1. *For each* $d \geq 4$*, there is an infinite family* $(\mathrm{TRP}_d[n])$, $n \in \mathbb{N}$ *of combinatorially distinct* d*-dimensional polytopes such that* $\dim \mathcal{RS}(\mathrm{TRP}_d[n]) \leq 76 + d(d+1)$ *for all* n*.*

Building on the family $(\mathrm{TRP}_4[n])$, we can use extension techniques, in particular Lawrence extensions (see for example [9]), to answer Problem I for all dimensions high enough.

Theorem II (Rigid transmitter polytopes, A.-Ziegler [1])**.** *There is an infinite family* $(\mathrm{RTP}_{81}[n])$, $n \in \mathbb{N}$ *of combinatorially distinct* 81*-dimensional polytopes, all of which are projectively unique.*

Again, we can immediately conclude:

Corollary 2. *For each* $d \geq 81$*, there is an infinite family* $(\mathrm{RTP}_d[n])$, $n \in \mathbb{N}$ *of combinatorially distinct* d*-dimensional polytopes, all of which are projectively unique.*

The hardest part of the proof of Theorem I (and Theorem II) goes into a geometric construction of a complex $\mathcal{T}_0$ that allows for the repeated attachment of 3-cubes in accordance with our construction technique. The pivotal structure for this initial complex $\mathcal{T}_0$ is formed by (weighted) Clifford tori, upon which we build the sequence of complexes $\mathcal{T}_n$, all of which are homeomorphic to $T^2 \times I$, and whose vertices are, in turn, distributed over several weighted Clifford tori in a symmetric fashion. For the study of $\mathcal{T}_0$ and its extensions $\mathcal{T}_n$, Santos [10] provided valuable intuition.

To ensure that the extensions $\mathcal{T}_n$ of $\mathcal{T}_0$ give rise to 4-polytopes, we use the notion of *convex position* complexes which is closely related to the theory of (locally) convex hypersurfaces, cf. [2, 4]. Convex position encodes the property of being the subcomplex of the boundary complex of a convex polytope. Using a careful adaption of the Alexandrov–van Heijenoort Theorem to manifolds with boundary, we prove that our complexes $\mathcal{T}_n$ are indeed in convex position, and consequently give rise to convex polytopes by considering the polytopes $\mathrm{TRP}_4[n] := \operatorname{conv} \mathcal{T}_n$.

To finish the proof, we then note that the realization space of the polytopes $\mathrm{TRP}_4[n]$ is naturally embedded into the realization space of $\mathcal{T}_n$, which in turn is embedded into the realization space of $\mathcal{T}_0$. In particular, $\dim \mathcal{RS}(\mathrm{TRP}_4[n]) \leq \dim \mathcal{RS}(\mathcal{T}_n) \leq \dim \mathcal{RS}(\mathcal{T}_0)$, and $\dim \mathcal{RS}(\mathrm{TRP}_4[n])$ is uniformly bounded. A more careful analysis gives the bound of Theorem I.

References

[1] K. Adiprasito and G. M. Ziegler, *On polytopes with low-dimensional realization spaces.* In preparation (2012).

[2] A. D. Aleksandrov, *Intrinsic geometry of convex surfaces.* OGIZ, Moscow-Leningrad, 1948.

[3] B. Grünbaum, *Convex polytopes.* Graduate Texts in Mathematics 221, Springer-Verlag, New York, second ed. 2003.

[4] J. van Heijenoort, *On locally convex manifolds.* Comm. Pure Appl. Math. **5** (1952), 223–242.

[5] G. Kalai, *Polytope skeletons and paths.* Handbook of Discrete and Computational Geometry (J. E. Goodman and J. O'Rourke, eds.), Chapman & Hall/CRC, Boca Raton, FL, second ed. 2004, 455–476.

[6] A. M. Legendre, *Éléments de géometrie.* Imprimerie de Firmin Didot, Paris 1794, twelfth ed. 1823 `http://archive.org/details/lmentsdegomtrie10legegoog`.

[7] P. McMullen, *Constructions for projectively unique polytopes.* Discrete Math. **14** (1976), 347–358.

[8] M. A. Perles and G. C. Shephard, *A construction for projectively unique polytopes.* Geometriae Dedicata **3** (1974), 357–363.

[9] J. Richter-Gebert, *Realization spaces of polytopes.* Lecture Notes in Mathematics 1643, Springer-Verlag, Berlin, 1996.

[10] F. Santos, *A counterexample to the Hirsch conjecture.* Ann. of Math. **176** (2012), 383–412.

[11] E. Steinitz and H. Rademacher, *Vorlesungen über die Theorie der Polyeder unter Einschluss der Elemente der Topologie.* Springer-Verlag, 1934.

[12] G. M. Ziegler, *Polytopes with low-dimensional realization spaces (joint work with K. Adiprasito).* Oberwolfach Rep. **8** (2011), 2522–2525.

Discrete complex analysis: conformal invariants without conformal invariance

Dmitry Chelkak

Dealing with some 2D lattice model and its scaling limit (e.g., with the 2D Brownian motion in a fixed planar domain, which can be realized as a limit of random walks on refining lattices $\delta\mathbb{Z}^2$), one usually works in the context when the lattice mesh δ tends to zero. Then, one can argue that a pre-limiting behavior of the model is sufficiently close to the limiting one, if δ is small enough, e.g., the random walks hitting probabilities (discrete harmonic measures) become close to the Brownian motion hitting probabilities (classical harmonic measure) as $\delta \to 0$. After re-scaling by δ^{-1}, such statements provide an information about random walk properties in (the bulk of) *large* discrete domains in $\mathbb{Z}^2$.

In this talk, we are interested in uniform estimates which hold true for *arbitrary* discrete domains, possibly having *many fiords and bottlenecks of various widths*, including very thin (several lattice steps) ones. Having in mind the classical geometric complex analysis as a guideline, we would like to construct its discrete version "staying on a microscopic level" (i.e., without any limit passage), which allows one to handle discrete domains by the same methods as continuous ones.

The main objects of our interest are discrete quadrilaterals, i.e. simply connected domains Ω with four marked boundary points a, b, c, d. Focusing on quadrilaterals, we are motivated by two reasons. First, in the classical theory this is the "minimal" configuration which has a nontrivial conformal invariant (e.g., all simply

connected domains with three marked boundary points are conformally equivalent due to the Riemann mapping theorem). Second, quadrilaterals are archetypical configurations for the 2D lattice models theory, where one often needs to estimate the probability of some crossing-type event between the opposite *boundary arcs* $[ab], [cd] \subset \partial\Omega$ of a discrete simply connected domain Ω.

Below we present a number of uniform double-sided estimates (1)–(3) relating discrete counterparts of several classical conformal invariants of a configuration $(\Omega; a, b, c, d)$: cross-ratios, random walk partition functions and extremal lengths.

Let Ω be a discrete domain (i.e., connected subset of $\mathbb{Z}^2$) and $A, B \subset \partial\Omega$. We denote by $\mathrm{Z}_\Omega(A; B)$ the *total partition function of the simple random walk* running from A to B inside Ω. Namely,

$$\mathrm{Z}_\Omega(A; B) = \mathrm{Z}_\Omega(B; A) \quad := \sum_{\gamma \in S_\Omega(a;b)} 4^{-\mathrm{Length}(\gamma)},$$

where $S_\Omega(A; B) = \{\gamma = (u_0 u_1 \dots u_n) : u_0 \in A,\ u_1, \dots, u_{n-1} \in \mathrm{Int}\Omega,\ u_n \in B\}$ is the set of all nearest-neighbor paths connecting A and B in Ω, and $\mathrm{Length}(\gamma) = n$.

Further, let Ω be a simply-connected discrete domain and $a, b, c, d \in \partial\Omega$ be four boundary points listed counterclockwise. We define their *discrete cross-ratios* by

$$\mathrm{X}_\Omega(a, b; c, d) := \left[\frac{\mathrm{Z}_\Omega(a; c) \cdot \mathrm{Z}_\Omega(b; d)}{\mathrm{Z}_\Omega(a; b) \cdot \mathrm{Z}_\Omega(c; d)}\right]^{\frac{1}{2}}, \quad \mathrm{Y}_\Omega(a, b; c, d) := \left[\frac{\mathrm{Z}_\Omega(a; d) \cdot \mathrm{Z}_\Omega(b; c)}{\mathrm{Z}_\Omega(a; b) \cdot \mathrm{Z}_\Omega(c; d)}\right]^{\frac{1}{2}}.$$

Note that the continuous analogue of the partition function $\mathrm{Z}_\Omega(a; b)$ for the upper half-plane $\Omega = \mathbb{H}$ (up to a multiplicative constant) is given by $(b - a)^{-2}$, so the quantities introduced above are discrete counterparts of the usual cross-ratios

$$x_{\mathbb{H}}(a, b; c, d) := \frac{(b-a)(d-c)}{(d-b)(c-a)}, \qquad y_{\mathbb{H}}(a, b; c, d) := \frac{(b-a)(d-c)}{(d-a)(c-b)}.$$

Moreover, for any *continuous* Ω, the corresponding x_Ω, y_Ω could be defined via a proper conformal mapping $\Omega \to \mathbb{H}$. In particular, one has the standard *identity* $x_\Omega^{-1} = 1 + y_\Omega^{-1}$ for any $(\Omega; a, b, c, d)$. Since in the *discrete* setup there is no appropriate notion of conformal invariance (for different subsets of the *fixed* grid), one cannot hope that this identity remains valid for discrete Ω's. Nevertheless, it turns out that the similar *uniform double-sided estimate* holds true:

$$\mathrm{X}_\Omega(a, b; c, d)^{-1} \asymp 1 + \mathrm{Y}_\Omega(a, b; c, d)^{-1}, \tag{1}$$

i.e., there exist two independent of Ω, a, b, c, d constants $C_1, C_2 > 0$ such that $C_1 \mathrm{X}_\Omega^{-1} \le 1 + \mathrm{Y}_\Omega^{-1} \le C_2 \mathrm{X}_\Omega^{-1}$ for all possible discrete quadrilaterals $(\Omega; a, b, c, d)$.

Further, note that the natural continuous analogues $z_\Omega([ab]; [cd])$ of the total partition functions $\mathrm{Z}_\Omega([ab]; [cd])$ are conformally invariant as well, and, for $\Omega = \mathbb{H}$, one has (up to a multiplicative constant)

$$z_{\mathbb{H}}([ab]; [cd]) = \log \frac{(c-a)(d-b)}{(d-a)(c-b)} = \log(1 + y_{\mathbb{H}}(a, b; c, d)).$$

Hence, this identity is fulfilled for any *continuous* quadrilateral $(\Omega; a, b, c, d)$. Again, it cannot survive on the discrete level, but one can prove that the similar uniform

double-sided estimate

$$\mathrm{Z}_\Omega([ab];[cd]) \asymp \log(1+\mathrm{Y}_\Omega(a,b;c,d)) \tag{2}$$

holds true for *discrete* quadrilaterals (with constants independent of $(\Omega;a,b,c,d)$).

In order to summarize our results, it is worthwhile to introduce the third quantity related to a discrete quadrilateral which is a well known discrete analogue of the *extremal length* notion. Let $E(\Omega)$ be the set of all edges of Ω. We define

$$\mathrm{L}_\Omega([ab];[cd]) := \sup_{w:E(\Omega)\to\mathbb{R}_+} \frac{\min_{\gamma\subset E(\Omega):[ab]\leftrightarrow[cd]} \left(\sum_{e\in\gamma} w(e)\right)^2}{\sum_{e\in E(\Omega)}(w(e))^2},$$

where min is taken over all nearest-neighbor paths γ connecting $[ab]$ and $[cd]$ in Ω and sup is over all nonnegative functions ("discrete metrics") $w : E(\Omega) \to \mathbb{R}_+$.

Note that one can easily estimate extremal lengths since for this purpose it is sufficient to take any "discrete metric" w_0 in Ω (possibly, having some natural geometric meaning) and estimate the corresponding ratio for this particular w_0. Our main results are summarized in the following

Theorem. *Let Ω be a simply connected discrete domain and boundary points $a,b,c,d \in \partial\Omega$ be listed in the counterclockwise order. Denote*

$$\mathrm{Y} := \mathrm{Y}_\Omega(a,b;c,d), \quad \mathrm{Z} := \mathrm{Z}_\Omega([ab];[cd]), \quad \mathrm{L} := \mathrm{L}_\Omega([ab];[cd]);$$

$$\mathrm{Y}' := \mathrm{Y}_\Omega(b,c;d,a), \quad \mathrm{Z}' := \mathrm{Z}_\Omega([bc];[da]), \quad \mathrm{L}' := \mathrm{L}_\Omega([bc];[da]).$$

Then, the following uniform estimates are fulfilled:

$$\mathrm{Y}\cdot\mathrm{Y}'=1 \qquad \begin{array}{lcl} \log(1+\mathrm{Y}) & \asymp \mathrm{Z} \le & \mathrm{L}^{-1} \\ \log(1+\mathrm{Y}') & \asymp \mathrm{Z}' \le & (\mathrm{L}')^{-1} \end{array} \qquad \mathrm{L}\cdot\mathrm{L}' \asymp 1 \tag{3}$$

Moreover, $\mathrm{Z}' \asymp (\mathrm{L}')^{-1}$, if $\mathrm{L}' \le \mathrm{const} < +\infty$ (or, equivalently, $\mathrm{L} \ge \mathrm{const} > 0$).

Finally, note that the most essential ingredient of our proofs is the asymptotics

$$G(u;u_0) = \frac{1}{2\pi}\log|u-u_0| + O(1)$$

of the free Green's function which is known (in a much more precise form) at least for the class of isoradial graphs. Thus, if this asymptotics is established for some class of planar graphs, one almost immediately has a "toolbox" described above (for this class of graphs) which allows one to use classical methods of geometric complex analysis more-or-less in the same style as in the usual continuous setup.

Fast Computation of Geodesic Distance via Linear Elliptic Equations

Keenan Crane
(joint work with Clarisse Weischedel and Max Wardetzky)

The geodesic distance ϕ to a point x on a Riemannian manifold M is typically characterized in terms of the nonlinear hyperbolic *eikonal equation* $|\nabla\phi| = 1$. We present an alternative formulation in terms of linear elliptic equations, which has important practical and numerical consequences. In particular, let Δ be the (negative-semidefinite) Laplace-Beltrami operator on M and let δ be a Dirac delta centered at x. The *heat kernel* is the solution to the heat equation

$$\dot{u} = \Delta u$$

with initial conditions $u_0 = \delta$. As observed by Varadhan [1],

$$\phi = \lim_{t\to 0} \sqrt{-4t \log u_t},$$

i.e., the geodesic distance can be recovered as the limit of a simple pointwise transformation applied to the heat kernel. In practice, however, it is difficult to obtain a precise numerical reconstruction of u_t.

Consider instead the single-step backward Euler approximation of the heat kernel given by the solution to the linear elliptic equation

$$(\mathrm{id} - t\Delta)v_t = \delta$$

for a fixed integration time t, where id is the identity operator. Since the function v_t is merely a crude approximation of the true heat kernel u_t, applying Varadhan's transformation no longer yields the geodesic distance. It can be shown, however, that $\lim_{t\to 0} v_t$ is a monotonically decreasing function of the distance to x, which means that ∇v_t will become parallel to the gradient of the distance function $\nabla\phi$ as $t \to 0$. Alternatively, if we define $X := -\nabla v_t/|\nabla v_t|$ then we have

$$\lim_{t\to 0} X = \nabla\phi,$$

since (as indicated by the eikonal equation) $\nabla\phi$ has unit length. For finite values of t the vector field X may not be integrable, but we can obtain a close approximation $\hat{\phi}$ of ϕ by solving the problem

$$\min_{\hat{\phi}} |\nabla\hat{\phi} - X|^2,$$

or equivalently, by solving

$$\Delta\hat{\phi} = \nabla \cdot X$$

which is a standard linear elliptic Poisson equation. These observations lead to the *heat method*, which can be used to obtain a consistent approximation $\hat{\phi}$ of geodesic distance (i.e., $\lim_{t\to 0} \hat{\phi} = \phi$):

Computationally this method is attractive because the linear equations from steps (I) and (III) can easily be prefactored and solved in parallel; step (II) is

Algorithm 1 The Heat Method

I. SOLVE $(\mathrm{id} - t\Delta)v_t = \delta$.
II. EVALUATE $X = -\nabla v_t / |\nabla v_t|$.
III. SOLVE $\Delta\hat{\phi} = \nabla \cdot X$.

a simple pointwise evaluation. Further discussion of the method (including discretization and numerics) can be found in [2].

REFERENCES

[1] S. Varadhan, *On the behavior of the fundamental solution of the heat equation with variable coefficients.* Communications on Pure and Applied Mathematics **20** (1967), 431–455.
[2] K. Crane, C. Weischedel, and M. Wardetzky, *Geodesics in heat.* arXiv:1204.6216v1.

Axioms for an Arbitrary (Discrete) Calculus with Dirichlet Problem and Hodge Decomposition

STEFAN W. VON DEYLEN

Consider am Riemannian manifold (M, g). The Dirichlet problem is to find minimisers of the Dirichlet energy $\mathbf{Dir}(u) = \langle du, du\rangle_{L^2} + \langle \delta u, \delta u\rangle_{L^2}$ inside an appropriate class of functions or differential forms. The (L^2-orthogonal) Hodge decomposition of any vector field α as

$$\alpha = d\phi + \delta\chi + \psi \qquad \text{such that } d\psi = 0, \delta\psi = 0$$

subject to some additional conditions on the boundary values of ϕ, χ and ψ, is strongly connected to the unique solvability of the Dirichlet problem. For both problems, it is well known that the space of Sobolev differential forms $H^1\Omega^k(M)$ is the appropriate choice of regularity, see [4].

There are several approaches to define "discrete exterior calculi", see e. g. [3, 2, 1]. Sometimes by interpolation properties, sometimes by mere discrete calculation, they show that the above properties of the continous calculus are reflected in their definitions.

We have asked ourselves for the "minimal set of definitions" that is fulfilled by all these discrete constructions as well as their smooth counterpart and propose the following:

Definition. *Suppose M is an n-dimensional compact, oriented cone manifold with boundary. An* ***exterior calculus*** *(G_k, Ω^k) consists of*

(a) collections $G_1, \dots, G_n$ of "integration domains": each $U \in G_k$ is a smooth k-dimensional submanifold of M such that ∂U can be covered by G_{k-1} domains.
(b) L^2-closed spaces $\Omega^0, \dots, \Omega^n$ of differential forms such that $\Omega^k \subset L^2\Omega^k(M)$ and each $\alpha \in \Omega^k$ is integrable on each $U \in G_k$.

This definition collects all objects that are needed to form a calculus. Let us add some purely notational definitions: A form is some $\alpha \in \Omega^k$ **weakly differentiable** if there is $d\alpha \in \Omega^{k+1}$ with

$$\int_U d\alpha = \int_{\partial U} \alpha \qquad \text{for all } U \in G_{k+1}.$$

Call $d\alpha$ the weak exterior derivative of α (if it is not unique, pick the one with least L^2 norm). The pointwise projection of α onto the tangent space of a lower-dimensional submanifold, e. g. ∂U, (the "tangential part") is denoted as $\mathbf{t}\,\alpha$, the projection onto the orthogonal complement (the "normal part") as $\mathbf{n}\,\alpha$.

Of course, one can construct very strange collections of forms and domains that do not have much to do with one another. As conditions for an exterior calculus to be "useable", we propose the following:

(a) the space $H^1\Omega^k$ of weakly differentiable Ω^k forms should be dense in Ω^k,
(b) there is a co-differential δ with $\langle \alpha, d\beta\rangle_{L^2} = \langle \delta\alpha, \beta\rangle_{L^2}$ if $\mathbf{t}\,\beta = 0$ or $\mathbf{n}\,\alpha = 0$,
(c) but if $\mathbf{n}\,\alpha \neq 0$, there is β with $\langle \alpha, d\beta\rangle_{L^2} \neq \langle \delta\alpha, \beta\rangle_{L^2}$ and vice versa for $\mathbf{t}\,\beta \neq 0$.

Remark that in general this co-differential δ is not neccessarily linked to the differential by the Hodge star, $\delta \neq *d*$.

Comparison. The fact that Ω^k may also be spaces of piecewise constant differential forms and yet admit a weak derivative in the above sense, as the Stokes' formula only has to hold on a very limited set of domains, has some implications for the comparison to other discrete calculi.

(1.) The FEEC (finite element exterior calculus) approach, cf. [1] and Ari Stern's abstract in this report, needs weakly differentiable forms in the usual Sobolev sense, e. g. piecewise smooth and globally continous forms. One way to see our definition is to make their approach applicable to the purely discrete approaches, e. g.:

(2.) The DEC (discrete exterior calculus) approach, cf. [2], does (at least in the first step) not define k-forms in the usual sense, but only numbers at k-cells. When some interpolation is chosen, mostly piecewise linear and globally continous (Whitney forms), Stokes' and Green's theorem do not neccessarily hold on the level of interpolating forms. But an appropriately chosen piecewise constant interpolation keeps both theorems valid, and it will be weakly differentiable in the above definition, thus admitting the results given below without extra proofs for the discrete setting.

Result. The reason that we consider these objects above as a "minimal set" of objects to form an exterior calculus is that a careful inspection of the Sobolev theory for the aforementioned problems, Dirichlet problem and the Hodge decomposition, e. g. from [4], shows that all their proofs will carry over. We especially emphasise that the following properties of any "useable" exterior calculus are proven by literally taking over the proofs from Sobolev theory:

Theorem. *Let (G_k, Ω^k) be a "useable" exterior calculus as above. Then hold for $\mathscr{H}^k := \{\alpha \in \Omega^k \mid \mathbf{Dir}(\alpha) = 0\}$:*

(a) ***Dirichlet problem:*** *For each* $f \in (\mathscr{H}^k_{\mathbf{t}})^\perp$, *there is a unique* $u \in (\mathscr{H}^k_{\mathbf{t}})^\perp_{\mathbf{t}}$ *with* $\langle d\alpha, d\psi\rangle + \langle \delta\alpha, \delta\psi\rangle = \langle f, \psi\rangle$ *for all* $\psi \in \Omega^k_{\mathbf{t}}$.
(b) ***Hodge decomposition:*** $\Omega^k = d(\Omega^{k-1}_{\mathbf{t}}) \oplus \delta(\Omega^{k+1}_{\mathbf{n}}) \oplus \mathscr{H}^k$
(c) *Friedrichs decomposition:* $\mathscr{H}^k = \mathscr{H}^k_{\mathbf{n}} \oplus \mathscr{H}^k \cap d(\Omega^{k-1}) = \mathscr{H}^k_{\mathbf{t}} \oplus \mathscr{H}^k \cap \delta(\Omega^{k+1})$
(d) $\ker d_k / \operatorname{im} d_{k-1} \simeq \mathscr{H}^k_{\mathbf{n}}$
(e) ***de Rham:*** *if* $\operatorname{span}_{\mathbb{R}}(G_k)$ *is a dense subspace of* $(\Omega^k)'$, *then* $\ker \partial_k / \operatorname{im} \partial_{k+1} \simeq \ker d_k / \operatorname{im} d_{k-1}$

References

[1] Arnold, D. N, Falk, R. S., and Winther R., *Finite element exterior calculus: From Hodge theory to numerical stability.* Bulletin of the AMS **47** (2010), pp. 281–354.
[2] Desbrun, M., Kanso, E., and Tong, Y., *Discrete differential forms for computational modeling.* In: ACM SIGGRAPH Asia 2008 courses, New York: ACM 2008, pp. 46–67.
[3] Polthier, K. and Preuss, E., *Variational approach to vector field decomposition.* In: Scientific Visualization (Proceedings of the Eurographics Workshop on Scientific Visualization Amsterdam 2000), Springer, Berlin 2000.
[4] Schwarz, G., *Hodge decomposition – A Method for Solving Boundary Value Problems.* Lecture Notes in Mathematics 1607, Berlin, Springer 1995.

Hirota equation and the quantum plane

Adam Doliwa

Hirota's discrete Kadomtsev–Petviashvili equation [5] may be considered as the Holy Grail of integrable systems theory, both on the classical and the quantum level [6]. Its geometric interpretation is provided [2] by *Desargues maps* (see Figure 1). These are the maps $\phi : \mathbb{Z}^K \to \mathbb{P}^M(\mathbb{D})$ of multidimensional integer lattice into projective space (over a division ring $\mathbb{D}$) subject to collinearity of all triplets of points $\phi(n)$, $\phi_{(i)}(n)$ and $\phi_{(j)}(n)$, $i \neq j$; here $\phi_{(i)}(n_1, \dots, n_i, \dots, n_K) = \phi(n_1, \dots, n_i + 1, \dots, n_K)$. We remark that the symmetry properties of Desargues maps are more transparent [3] in the language of the A_K root lattice and of the corresponding affine Weyl group.

Geometric integrability of the maps follows from the celebrated Desargues theorem. In algebraic terms the nonlinear system generated by Desargues maps (a non-commutative Hirota equation) can be decomposed [4] into reiterated application of two maps, which are solutions of the functional pentagon equation. The simpler one $W : \mathbb{D}^2 \times \mathbb{D}^2 \ni ((x_1, y_1), (x_2, y_2)) \dashrightarrow ((\tilde{x}_1, \tilde{y}_1), (\tilde{x}_2, \tilde{y}_2)) \in \mathbb{D}^2 \times \mathbb{D}^2$

$$\tilde{x}_1 = x_2 + x_1 y_2, \qquad \tilde{y}_1 = y_1 y_2 \tag{1}$$

$$\tilde{x}_2 = -y_1 x_1^{-1} x_2, \qquad \tilde{y}_2 = y_2 + x_1^{-1} x_2 \tag{2}$$

is related to collinearity of four points. We stress that the functional pentagon equation

$$W_{12} \circ W_{23} = W_{23} \circ W_{13} \circ W_{12}, \qquad \text{in} \qquad \mathbb{D}^2 \times \mathbb{D}^2 \times \mathbb{D}^2 \tag{3}$$

is satisfied without any assumptions about commutativity of the multiplication.

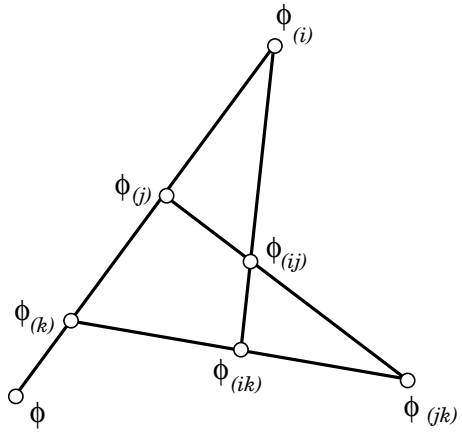

FIGURE 1. Desargues map condition and the Veblen configuration

The second map $W^G : \mathbb{D}^2 \times \mathbb{D}^2 \dashrightarrow \mathbb{D}^2 \times \mathbb{D}^2$

$$u_1' = Gw_1, \qquad w_1' = w_2 w_1$$
$$u_2' = -u_2 w_1 u_1^{-1}, \qquad w_2' = G w_1 u_1^{-1}$$

contains a free gauge parameter G, and is directly related to Desargues configuration. The pentagonal property of the map follows from the symmetry of the configuration; on the algebraic level the gauge parameters of the corresponding five maps have to be suitably adjusted.

We present also a path to the corresponding solutions of the quantum pentagon equation [1]. In doing the reduction from "noncommutative to quantum" we elucidate [4] the role of the ultra-locality principle (the tensor product structure) which leads to the Weyl commutation relations

$$xy = qyx$$

of the quantum plane $\mathbb{K}_q[x, y]$. Moreover, the pentagonal property of the map W implies coassociativity of the coproduct $\Delta : \mathbb{K}_q[x, y] \to \mathbb{K}_q[x, y] \otimes \mathbb{K}_q[x, y]$

$$\Delta(x) = 1 \otimes x + x \otimes y, \qquad \Delta(y) = y \otimes y, \tag{4}$$

which should be compared with equation (1). From that it follows the Hopf algebra structure of the extended quantum plane $\mathbb{K}_q[x, y, y^{-1}]$.

REFERENCES

[1] S. Baaj, G. Skandalis, *Unitaires multiplicatifs et dualité pour les produits croisés de C^*-algèbres.* Ann. Sci. École Norm. Sup. **26** (1993), 425–488.

[2] A. Doliwa, *Desargues maps and the Hirota–Miwa equation.* Proc. R. Soc. A **466** (2010), 1177–1200.

[3] A. Doliwa, *The affine Weyl group symmetry of Desargues maps and of the non-commutative Hirota–Miwa system.* Phys. Lett. A **375** (2011), 1219–1224.

[4] A. Doliwa, S. M. Sergeev, *The pentagon relation and incidence geometry.* arXiv:1108.0944.
[5] R. Hirota, *Discrete analogue of a generalized Toda equation.* J. Phys. Soc. Jpn. **50** (1981), 3785–3791.
[6] A. Kuniba, T. Nakanishi, J. Suzuki, *T-systems and Y-systems in integrable systems.* J. Phys. A: Math. Theor. **44** (2011), 103001 (146pp).

Discrete complex analysis on quad-graphs

Felix Günther
(joint work with Alexander I. Bobenko)

We deal with a linear discretization of complex analysis on quad-graphs. Discrete holomorphic functions on the square lattice were studied by Isaacs [7], where he proposed two different definitions for holomorphicity. One of them was reintroduced by Ferrand [6] and studied extensively by Duffin [4], who extended the notion of discrete holomorphicity to rhombic lattices [5]. The investigation of discrete complex analysis on rhombic lattices was resumed by Mercat [9], Kenyon [8], Chelkak and Smirnov [3]. For a survey on the theory of discrete complex analysis based on circle patterns and its relation to the linear theory, see the book of Bobenko and Suris [2].

Our setting is a bipartite quad-graph Λ corresponding to a strongly regular and locally finite cell decomposition of a Riemann surface consisting of quadrilaterals only. Mainly, we are interested in bipartite quad-graphs embedded in the complex plane. We denote by Γ respectively Γ^* the maximal independent sets of Λ. In addition to the graph Λ, its dual $\diamondsuit := \Lambda^*$ will come up in the definitions of discrete derivatives.

Being consistent with the previous definitions of discrete holomorphicity, a function $H : \Lambda \to \mathbb{C}$ is *discrete holomorphic* on the face $z \in \diamondsuit$, iff

$$\frac{H(u_+) - H(u_-)}{u_+ - u_-} = \frac{H(w_+) - H(w_-)}{w_+ - w_-}$$

for the two diagonals u_-u_+ and w_-w_+ of z. Based on this notion of holomorphicity, we generalize the *discrete derivatives* $\partial, \bar\partial$ of [3] to arbitrary quadrilaterals. These discrete derivatives map functions on Λ to functions on $\diamondsuit$ or vice versa. As in the rhombic setting, we can find *discrete primitives* of discrete holomorphic functions on simply-connected domains of $\diamondsuit$.

For functions on Λ, we show the factorization $4\partial\bar\partial = 4\bar\partial\partial = \triangle$ where $\triangle$ is the *discrete Laplacian* introduced by Mercat [10] and studied by Skopenkov [11]. As a corollary, ∂H is discrete holomorphic if $H : \Lambda \to \mathbb{C}$ is *discrete harmonic*, i.e. $\triangle H \equiv 0$. Also, the real and the imaginary part of a discrete holomorphic function $H : \Lambda \to \mathbb{C}$ are discrete harmonic. Moreover, if H is discrete holomorphic on a simply-connected domain, the imaginary part of H is determined uniquely by its real part up to two additive constants on Γ and Γ^*. In particular, a discrete holomorphic and purely real or purely imaginary function H on a simply-connected domain is constant on Γ and constant on Γ^*.

Skopenkov proved existence and uniqueness of solutions to the discrete Dirichlet boundary value problem [11]. Basing on this result, we prove surjectivity of the operators $\partial, \bar{\partial}, \Diamond$ on discrete domains homeomorphic to a disk or the plane. Especially, *discrete Green's functions* $G(\cdot; v_0) : \Lambda \to \mathbb{R}$ and *discrete Cauchy kernels* $K(\cdot, v_0) : \Diamond \to \mathbb{C}$ and $K(\cdot, z_0) : \Lambda \to \mathbb{C}$ exist for all $v_0 \in \Lambda$ and $z_0 \in \Diamond$ in the case that Λ discretizes the complex plane. For all $v \in \Lambda$ and $z \in \Diamond$, these functions fulfill

$$G(v_0; v_0) = 0 \text{ and } \triangle G(v; v_0) = \frac{1}{2\mu_\Lambda(v_0)}\delta_{vv_0},$$
$$\bar{\partial} K(\cdot; z_0) = \delta_{zz_0}\frac{\pi}{\mu_\Diamond(z_0)} \text{ and } \bar{\partial} K(\cdot; v_0) = \delta_{vv_0}\frac{\pi}{\mu_\Lambda(v_0)}.$$

Here δ is the Kronecker delta, and $\mu_\Lambda(v_0)$ are $\mu_\Diamond(z_0)$ are geometric weights associated to vertices of Λ and $\Diamond$ which already appear in the definitions of ∂ and $\bar{\partial}$. Note that we do not require any certain asymptotic behavior. However, we construct discrete Green's functions and Cauchy kernels with asymptotics analogous to the rhombic [3, 8] and close to the smooth case if all quadrilaterals are parallelograms with bounded interior angles and bounded ratio of side lengths. The construction of these functions is closely related to discrete complex analysis on quasicrystallic parallelogram-graphs [1] and uses the connection to discrete integrable systems [2].

To state discrete Cauchy formulas in a simpler way than in [3], we introduce the *medial graph* X of Λ which is defined as follows. The vertex set is given by the set of midpoints of all edges of Λ and two vertices are adjacent iff the corresponding edges belong to the same face and have a vertex in common. The set of faces of X is in bijective correspondence with the vertex set $\Lambda \cup \Diamond$: A face corresponding to a vertex v of Λ consists of the midpoints of all edges incident to v and a quadrilateral face corresponding to a face z of $\Diamond$ consists of the four midpoints of edges belonging to z. So given two functions $F : \Diamond \to \mathbb{C}$ and $H : \Lambda \to \mathbb{C}$, we can define a product $F \cdot H$ on the edges of X in a canonical way. Such functions can then be integrated along paths of edges of X.

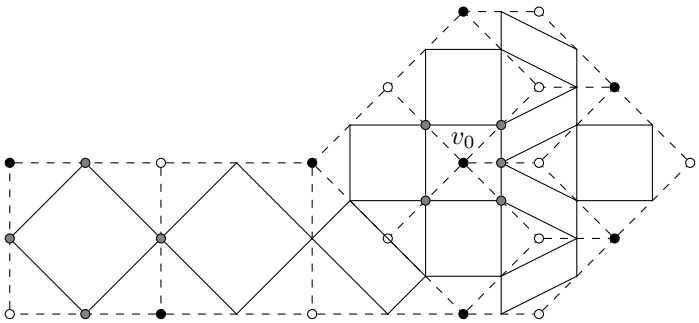

FIGURE 1. Bipartite quad-graph Λ (dashed) with medial graph X

Note that choosing $F \equiv 1$ or $H \equiv 1$, F respectively H is discrete holomorphic iff all closed discrete line integrals of $1 \cdot H$ respectively $F \cdot 1$ vanish, yielding a

discrete Morera's theorem. Also, all closed discrete line integrals of $F \cdot H$ vanish if F and H are both discrete holomorphic. Though, $F \cdot H$ is not everywhere discrete holomorphic in the sense of the theory above. More precisely, $F \cdot H$ is defined on the vertices of the medial graph of X, which is the dual of a bipartite quad-graph having $\Lambda \cup \Diamond$ as one maximal independent vertex set and the midpoints of edges of Λ as the other. But in general, $F \cdot H$ is discrete holomorphic on the vertices of $\Lambda \cup \Diamond$ only.

Let $F : \Diamond \to \mathbb{C}$ and $H : \Lambda \to \mathbb{C}$ be discrete holomorphic, and $v_0 \in \Lambda$, $z_0 \in \Diamond$. If $K(\cdot, z_0) : \Lambda \to \mathbb{C}$ and $K(\cdot, v_0) : \Diamond \to \mathbb{C}$ are discrete Cauchy kernels, then for any discrete contour C_{z_0} or C_{v_0} on the medial graph X surrounding z_0 respectively v_0 once in counterclockwise order (e.g. the paths determined by the gray vertices in Figure 1), the *discrete Cauchy formula* holds true:

$$F(z_0) = \frac{1}{2\pi i} \oint_{C_{z_0}} F \cdot K(\cdot; z_0),$$

$$H(v_0) = \frac{1}{2\pi i} \oint_{C_{v_0}} K(\cdot; v_0) \cdot H.$$

If additionally C_{z_0} does not pass through any vertex incident to z_0, then

$$\partial H(z_0) = \frac{1}{2\pi i} \oint_{C_{z_0}} -\partial K(\cdot; z_0) \cdot H.$$

In the special case of the $\mathbb{Z}^2$-lattice of a skew coordinate system in the complex plane, $\Diamond \cong \Lambda$ and all derivatives of a discrete holomorphic functions are discrete holomorphic themselves. We derive discrete Cauchy formulas for all discrete derivatives and show that the nth derivative of the discrete Cauchy kernel with asymptotics $O(x^{-1})$ has asymptotics $O(x^{-(n+1)})$.

References

[1] A.I. Bobenko, C. Mercat and Yu. B. Suris, *Linear and nonlinear theories of discrete analytic functions. Integrable structure and isomonodromic Green's function.* J. Reine Angew. Math. **583** (2005), 117–161.

[2] A.I. Bobenko and Yu.B. Suris, *Discrete differential geometry: integrable structures.* Grad. Stud. Math. 98, AMS, Providence 2008.

[3] D. Chelkak and S. Smirnov, *Discrete complex analysis on isoradial graphs.* Adv. Math. **228** (2011), 1590–1630.

[4] R.J. Duffin, *Basic properties of discrete analytic functions.* Duke Math. J. **23** (1956), 335–363.

[5] R.J. Duffin, *Potential theory on a rhombic lattice.* J. Comb. Th. **5** (1968), 258–272.

[6] J. Ferrand, *Fonctions préharmoniques et fonctions préholomorphes.* Bull. Sci. Math. (2) **68** (1944), 152–180.

[7] R.Ph. Isaacs, *A finite difference function theory.* Univ. Nac. Tucumán. Revista A **2** (1941), 177–201.

[8] R. Kenyon, *The Laplacian and Dirac operators on critical planar graphs.* Invent. math. **150** (2002), 409–439.

[9] C. Mercat, *Discrete Riemann surfaces and the Ising model.* Commun. Math. Phys. **218** (2001), 177–216.
[10] C. Mercat, *Discrete complex structure on surfel surfaces.* Proceedings of the 14th IAPR international conference on Discrete geometry for computer imagery (2008), 153–164.
[11] M. Skopenkov, *Boundary value problem for discrete analytic functions.* arXiv:1110.6737 (2011).

Consistent discretizations of the Laplace–Beltrami operator and the Willmore energy of surfaces

Klaus Hildebrandt
(joint work with Konrad Polthier)

A fundamental aspect when translating classical concepts from smooth differential geometry, such as differential operators or geometric functionals, to corresponding discrete notions is consistency. A discretization is consistent if the discrete operator or functional converges to its smooth counterpart in the limit of refinement. Here, we are concerned with the construction of consistent counterparts to the Laplace–Beltrami operator and the Willmore energy on polyhedral surfaces in $\mathbb{R}^3$. Our starting point is the weak form of the Laplace–Beltrami operator (LBO) on a smooth surface M. This is the continuous linear operator that maps any $u \in H^1(M)$ to the distribution $\Delta u \in H^1(M)'$ that is given by

$$\langle \Delta u | \varphi \rangle = -\int_M g(\operatorname{grad} u, \operatorname{grad} \varphi)\, \mathrm{d}vol \tag{1}$$

for all $\varphi \in H^1(\mathcal{M})$. Here $H^1(M)$ denotes the Sobolev space of functions whose first derivative is square integrable, $H^1(M)'$ is the (topological) dual space, and $\langle \cdot | \cdot \rangle$ denotes the pairing of $H^1(M)'$ and $H^1(M)$. This operator can be rigorously defined on polyhedral surfaces, and, in [1], convergence of this operator to its smooth counterpart in an appropriate operator norm was shown. To discretize the operator, we restrict u and φ to be functions in the finite dimensional subspace S_h of H^1 consisting of continuous functions that are piecewise linear over the triangles. Then, the discrete weak LBO is a map from S_h to S_h' (the dual space of S_h). It can be used to discretize second order differential equation on surfaces, and convergence of solutions of discrete Dirichlet problems of Poisson's equation was shown in [2]. In contrast to the weak form, discretizations of the strong LBOs are endomorphisms of S_h. Based on the discrete weak LBO, different constructions of discrete strong LBOs are used in practice, but none of them was proven to be consistent and counterexamples to pointwise convergence have been reported.

Here, we introduce a consistent discretization of the strong LBO. As a tool for the construction, we use functions that we call r-local functions.

Definition 1. *Let $\mathcal{M}$ be a smooth or a polyhedral surface in $\mathbb{R}^3$, and let C_D be a positive constant. For any $x \in \mathcal{M}$ and $r \in \mathbb{R}^+$, we call a function $\varphi : \mathcal{M} \mapsto \mathbb{R}$* r-local *at x (with respect to C_D) if the criteria*

(D1) $\varphi \in W^{1,1}(\mathcal{M})$,

(D2) $\varphi(y) \geq 0$ *for all* $y \in \mathcal{M}$,

(D3) $\varphi(y) = 0$ *for all* $y \in \mathcal{M}$ *with* $d_{\mathcal{M}}(x, y) \geq r$,

(D4) $\|\varphi\|_{L^1} = 1$, *and*

(D5) $|\varphi|_{W^{1,1}(\mathcal{M})} \leq \frac{C_D}{r}$

are satisfied.

A function that is r-local at $x \in M$ can be used to approximate the function value at x of a function f through the integral $\int_M f\,\varphi\,\mathrm{d}vol$. In this sense, r-local functions are approximations of the delta distribution.

Lemma 1. *Let $\varphi \in L^1(M)$ satisfy properties (D2), (D3), and (D4) of Definition 1 for some $x \in M$ and $r \in \mathbb{R}^+$, and let $f \in C^1(M)$. Then, the estimate*

$$\left| f(x) - \int_M f\,\varphi\; dvol \right| \leq \|grad\;\; f\|_{L^\infty}\; r \tag{2}$$

holds.

Certain functions φ even exhibit a higher approximation order: there r-local functions φ that satisfy

$$\left| f(x) - \int_M f\,\varphi\,\mathrm{d}vol \right| \leq C\,r^2, \tag{3}$$

where C depends on M and the second derivatives of f.

A function in S_h is uniquely determined by its function values at the vertices. Assuming a total ordering of the vertices, the function values can be listed in a vector, which is called the nodal vector. We will describe the discrete LBOs by their action on the nodal vectors. Let $\{\varphi_i\}_{i\in\{1,2,..n\}}$ be a set of functions such that every φ_i is r-local at the vertex $v_i \in M_h$. Then, we define the discrete Laplace–Beltrami operator $\Delta_{M_h}^{\{\varphi_i\}}$ associated to $\{\varphi_i\}$ as

$$\Delta_{M_h}^{\{\varphi_i\}} : S_h \mapsto S_h$$
$$\begin{pmatrix} u_h(v_1) \\ u_h(v_2) \\ \dots \\ u_h(v_n) \end{pmatrix} \mapsto \begin{pmatrix} \langle \Delta_{M_h} u_h | \varphi_1 \rangle \\ \langle \Delta_{M_h} u_h | \varphi_2 \rangle \\ \dots \\ \langle \Delta_{M_h} u_h | \varphi_n \rangle \end{pmatrix}.$$

For each φ_i there is a constant $C_{D,i}$ such that (D5) of Definition 1 is satisfied. In the following, we refer to the maximum of the $C_{D,i}$ as the constant C_D of $\{\varphi_i\}$.

For the proof of consistency of the discrete operators, we consider a polyhedral surface M_h that is closely inscribed to a smooth surface M, *i. e.* the vertices of M_h lie on M, M_h is in the reach of M, and the restriction to M_h of the orthogonal project onto M is a bijection. We denote the restricted orthogonal projection by π. Furthermore, for a smooth function u on M, we denote by u_h the function in S_h that interpolates the function values of u at the vertices of M_h.

Theorem 1. *Let M be a smooth surface in $\mathbb{R}^3$, and let u be a smooth function on M. Then there exists a $h_0 \in \mathbb{R}^+$ such that for every pair consisting of a polyhedral surface M_h that is closely inscribed to M and satisfies $h < h_0$ and a set of functions $\{\varphi_i\}_{i\in\{1,2,..n\}}$ such that every φ_i is r-local at the vertex $v_i \in M_h$ with $r = \sqrt{h}$, the estimate*

$$\sup_{y\in M_h} \left|\Delta u(\pi(y)) - \Delta_{M_h}^{\{\varphi_i\}} u_h(y)\right| \leq C\sqrt{h} \tag{4}$$

holds, where $u_h \in S_h(M_h)$ is the interpolant of u. If every $\varphi_i \circ \pi^{-1}$ satisfies (3) and $r = h^{\frac{1}{3}}$, then we have

$$\sup_{y\in M_h} \left|\Delta u(\pi(y)) - \Delta_{M_h}^{\{\varphi_i\}} u_h(y)\right| \leq C\, h^{\frac{2}{3}}. \tag{5}$$

The constants C depend only on M, u, h_0, the shape regularity ρ of M_h, and the constant C_D of $\{\varphi_i\}$.

We plan to use the discrete LBOs to discretize forth-order problems on surfaces. As a first step in this direction, we derived a consistent discretization of the Willmore energy. The Willmore energy of a smooth surface M in $\mathbb{R}^3$ is

$$W(M) = \int_M H^2 \mathrm{d}vol, \tag{6}$$

where H denotes the mean curvature of M. It is connected to the Laplace–Beltrami operator through the mean curvature vector field $\mathbf{H} = HN = \Delta I$. It follows that the Willmore energy of M equals the squared L^2-norm of ΔI.

Let $I_{M_h} : M_h \mapsto \mathbb{R}^3$ denote the embedding of the polyhedral surface M_h. Each of the three components of I_{M_h} is a function in S_h. Therefore, we can define the discrete Willmore energy of M_h and $\{\varphi_i\}$ as

$$W_{M_h}^{\{\varphi_i\}}(M_h) = \|\Delta_{M_h}^{\{\varphi_i\}} I_{M_h}\|^2_{L^2(M_h)}.$$

The following theorem shows consistency of the discrete Willmore energies.

Theorem 2. *Let M be a smooth surface in $\mathbb{R}^3$. Then there exists a $h_0 \in \mathbb{R}^+$ such that for every pair consisting of a polyhedral surface M_h that is inscribed to M and satisfies $h < h_0$ and a set of functions $\{\varphi_i\}_{i\in\{1,2,..n\}}$ such that every φ_i is r-local at the vertex $v_i \in M_h$ with $r = \sqrt{h}$, the estimate*

$$\left|W(M) - W_{M_h}^{\{\varphi_i\}}(M_h)\right| \leq C\sqrt{h}$$

holds. If every $\hat{\varphi}_i$ satisfies (3) and $r = h^{\frac{1}{3}}$, then we have

$$\left|W(M) - W_{M_h}^{\{\varphi_i\}}(M_h)\right| \leq C\, h^{\frac{2}{3}}.$$

The constants C depend only on M, h_0, the shape regularity ρ of M_h, and the constant C_D of $\{\varphi_i\}$.

Proofs to the theorems can be found in [3].

References

[1] K. Hildebrandt, K. Polthier, M. Wardetzky, *On the convergence of metric and geometric properties of polyhedral surfaces.* Geometricae Dedicata **123** (2006), 89–112.

[2] G. Dziuk, *Finite elements for the Beltrami operator on arbitrary surfaces.* In: S. Hildebrandt and R. Leis (Eds.), Partial Differential Equations and Calculus of Variations, Springer-Verlag 1988, 142–155.

[3] K. Hildebrandt and K. Polthier. *On approximation of the Laplace–Beltrami operator and the Willmore energy of surfaces.* Computer Graphics Forum, **30** (2011), 1513–1520.

Discrete focal surfaces and geodesics

Wolfgang K. Schief and Tim Hoffmann

Voss surfaces are surfaces which can be parametrized by two conjugate families of geodesics [1]. However, there exists another characterization of Voss surfaces which is intimately related to their canonical discretization as recorded by Sauer [2] and Wunderlich [3]. Thus, Voss surfaces are reciprocal parallel to surfaces of constant negative Gaussian curvature (K surfaces). These K surfaces admit a natural discretization [2, 3] which is linked to the discrete Voss surfaces proposed by Sauer and Graf [4] via a discrete analogue of reciprocal parallelism. In fact, the latter may be interpreted in terms of equilibrium of forces acting along the edges of discrete Voss sufaces [3] or infinitesimal isometric deformations of discrete Voss surfaces [4]. It turns out that discrete Voss surfaces admit finite isometric deformations, which constitutes the counterpart of a well-known property in the classical setting. However, it is by no means obvious in what sense the mesh polygons of discrete Voss surfaces constitute discrete geodesics on the surface.

It is a known fact that a family of lines of curvature on a surface is mapped to a family of geodesics on the corresponding focal surface, that is, the loci of the centre of curvature associated with the family of lines of curvature. Moreover, the other family of lines of curvature is mapped to lines which are conjugate to the geodesics. Thus, a Voss surface can be characterized as being a focal surface of two different surfaces which are parametrized in terms of curvature coordinates with the two corresponding families of geodesics being mutually conjugate as mentioned above. The standard discretization of conjugate nets [5] is given by quadrilateral meshes with planar faces (pq-meshes). These constitute discrete curvature line nets if the quadrilaterals are circular and, modulo an arbitrary choice of one vertex normal, an associated vertex Gauss map, which itself constitutes a circular mesh, may be defined uniquely. In this setup, as in the classical case, there exist canonical focal points and one is therefore naturally led to an investigation of the properties of the resulting focal meshes. It is noted that focal meshes for circular and conical meshes have been considered in [7].

It turns out that the focal meshes associated with circular meshes are discrete conjugate and that one can characterize the fact that a mesh is a focal mesh of a circular mesh by a compact condition on the four angles made by an edge of one family of coordinate polygons and the four edges of the other family of coordinate polygons which emanate from the two vertices of the edge. This angle condition

encodes the property that the four associated tangent directions incident with the edge are the vertices of a circular quadrilateral when thought of as points on the unit sphere and we refer to this property as geodesic-circular. The simplest example of discrete surfaces which possess this property is given by discrete rotationally symmetric pq-meshes. The condition of a pq-mesh to be geodesic-circular in both lattice directions can now be encoded in the property that these normalized tangent directions form two circular meshes on the unit sphere which are related by a discrete Laplace transform projected onto the sphere. Remarkably, this novel discretization of Voss surfaces includes Sauer and Graf's "classical" discrete Voss surfaces in the special case that all dihedral angles in any of the two lattice directions are the same.

In general, classical discrete Voss surfaces are defined by the requirement that opposite angles at each vertex star be equal. In order to gain more insight into the classical discrete Voss surfaces which are not captured by our novel discretization, we now consider a different discretization of curvature line nets, namely conical meshes (see [6]). A conical mesh is a pq-mesh such that the faces incident to each vertex are in oriented contact with a cone of revolution originating in that vertex. Here, the key property is "oriented contact". Thus, a mesh is conical or, better, curvature-conical, iff, at each vertex, the two sums of opposite angles are the same. However, there exist other ways in which a cone can touch the four faces (or the corresponding planes) incident to a vertex. For instance, we call a mesh geodesic-conical iff, at each vertex, the sum of two neighbouring angles coincide with the sum of the other two. In these and the remaining cases, the planes of the faces around a vertex touch a common cone of revolution but with different orientations. Again, discrete rotationally symmetric pq-meshes can serve as an example and the classical discrete Voss surfaces constitute meshes that are geodesic-conical in both lattice directions.

There exists a well-known connection between conical and (curvature-)circular meshes. Thus, for any conical mesh, one can construct a two-parameter family of circular meshes with vertices on the faces of the conical mesh and the axes of the circles coinciding with the axes of the cones. In the curvature-conical case, the conical and the circular nets essentially discretize the same surface. However, in the geodesic-conical case, the conical mesh should be viewed as a focal mesh of the circular one. In this manner, the classical discrete Voss surfaces constitute simultaneously discrete focal surfaces of two different circular meshes as mentioned in the preceding.

References

[1] A. Voss, *Über diejenigen Flächen, auf denen zwei Scharen geodätischer Linien ein conjugirtes System bilden*, Sitzungsber. Bayer. Akad. Wiss., math.-naturw. Klasse (1888) 95–102.

[2] R. Sauer, *Parallelogrammgitter als Modelle für pseudosphärische Flächen*, Math. Z. **52** (1950) 611–622.

[3] W. Wunderlich, *Zur Differenzengeometrie der Flächen konstanter negativer Krümmung*, Österreich. Akad. Wiss. Math.-Nat. Kl. S.-B. II **160** (1951) 39–77.

[4] R. Sauer and H. Graf, *Über Flächenverbiegungen in Analogie zur Verknickung offener Facettenflache*, Math. Ann. **105** (1931) 499–535.
[5] R. Sauer, *Wackelige Kurvennetze bei einer infinitesimalen Flächenverbiegung*, Math. Ann. **108** (1933) 673–693.
[6] Y. Liu, H. Pottmann, J. Wallner and Y.-L. Wang, *Geometric modeling with conical meshes and developable surfaces.* ACM Trans. Graphics **25** (2006), 681–689.
[7] H. Pottmann and J. Wallner, *The focal geometry of circular and conical meshes.* Adv. Comput. Math. **29** (2008), 249–268.

Flexible Kokotsakis polyhedra and elliptic functions

Ivan Izmestiev

A Kokotsakis polyhedron with an n-gonal base is a polyhedral surface in $\mathbb{R}^3$ that consists of one n-gon, n quadrilaterals attached to the sides of the n-gon, and n triangles attached to the vertices of the n-gon and to the adjacent sides of the quadrilaterals. A Kokotsakis polyhedron with a quadrangular base can be viewed as a part of an infinite polyhedral surface combinatorially isomorphic to the square grid: see Figure 1, left. Polyhedral surfaces of this kind are being intensively studied.

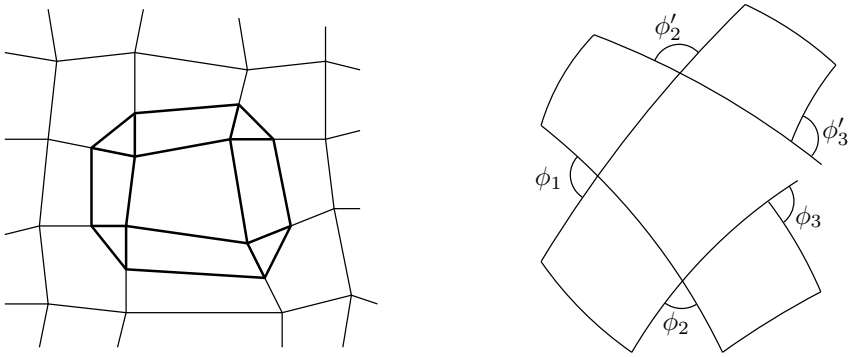

Figure 1. A Kokotsakis polyhedron as a part of a quad-surface; the corresponding spherical linkage.

Kokotsakis (1932) characterized infinitesimally flexible Kokotsakis polyhedra and gave some examples of flexible polyhedra with quadrangular base. Other examples were found by Graf and Sauer, and recently by Schief and (independently) Stachel.

In this talk we describe an approach that allows to characterize all flexible Kokotsakis polyhedra with a quadrangular base. We show that any flexible polyhedron belongs to one of the known classes: Kokotsakis, Graf-Sauer, or Schief-Stachel.

Consider the spherical link of a vertex of the polyhedron. This is a spherical quadrilateral, and an isometric deformation of the polyhedron results in an isometric deformation of this spherical quadrilateral. The angles of the spherical link

correspond to the dihedral angles of the polyhedron, thus the links of adjacent vertices have a pair of equal angles. All four spherical links together form a spherical linkage pictured on Figure 1, right. The polyhedron is flexible if and only if during the motion of this spherical linkage the angles ϕ_3 and ϕ_3' remain equal.

By introducing new variables

$$z_k = \tan \frac{\phi_k}{2}$$

one finds a polynomial relation between z_1 and z_2:

$$c_{22} z_1^2 z_2^2 + c_{20} z_1^2 + c_{02} z_2^2 + 2c_{11} z_1 z_2 + c_{00} = 0 \tag{1}$$

By writing a similar polynomial for z_2 and z_3 and excluding z_2 one finds a polynomial relation $P_{13}(z_1, z_3) = 0$. In a similar way, by means of z_2', one finds a polynomial relation $P_{13}'(z_1, z_3') = 0$. Since $z_3 = z_3'$, a necessary and sufficient condition for flexibility is that polynomials P_{13} and P_{13}' have a common factor. This approach was proposed by Stachel and partially realized by Nawratil.

We study the dependence between z_1 and z_3 from the viewpoint of branched covers and monodromy. Namely, the equations $P_{13}(z_1, z_3) = 0$ and $P_{13}'(z_1, z_3') = 0$ determine two branched covers over $\mathbb{C}P^1 \ni z_1$, and a necessary condition for flexibility is that a component of one cover coincides with a component of the other. By analyzing all possible monodromies we show that this coincidence can take place only in one of the known cases.

The solution set of (1) is in general an elliptic curve. The variables z_1 and z_2 correspond to two functions on this curve that differ by a shift along the curve and a multiplication with a constant. The recently found examples of Schief and Stachel appear when all four elliptic curves at the interior vertices of the polyhedron have the same modulus, the functions z_i have the same amplitudes on the two curves where they are defined, and the sum of four shifts is a period of the curve.

The Geometry of Light Transport Theory

Christian Lessig

Light transport theory, also known as radiative transfer, describes the propagation of electromagnetic energy at the short wavelength limit when polarization effects are neglected. Applications of the theory are for example in computer graphics, medical imaging, climate science, and astrophysics. Despite the practical importance, the mathematical foundations of the theory are still those introduced in the 18^{th} century and its physical basis is phenomenological, with little connection to more fundamental theories of light in physics. Following recent literature that develops an approach akin to inverse quantization to study quadratic observables of partial differential equations [9, 1], we show that a geometric formulation of light transport theory can be obtained rigorously and naturally from classical electromagnetic theory, and we initiate a study of this geometric structure.

Maxwell's equations, Hamilton's equations for electromagnetic field theory, are

$$\frac{\partial}{\partial t}\begin{pmatrix}\vec{E}\\ \vec{H}\end{pmatrix}=\begin{pmatrix}0 & \frac{1}{\varepsilon}\nabla\times\\ \frac{1}{\mu}\nabla\times & 0\end{pmatrix}\begin{pmatrix}\vec{E}\\ \vec{H}\end{pmatrix}$$

and in operator notation they can be written as

$$\dot{F}^{\epsilon}=P^{\epsilon}F^{\epsilon}$$

where $F^{\epsilon}=(\vec{E},\vec{H})^T$ is the Faraday vector and P^{ϵ} is the the Maxwell operator. The scale parameter $\epsilon=\lambda/\lambda_n$ in the above equation is proportional to the wavelength of light λ and it vanishes at the short wavelength limit when $\lambda\to 0$. To study the time evolution of quadratic obervables such as the energy density

$$\mathcal{E}(q)=\|\vec{F}\|^2_{\varepsilon,\mu}=\frac{\varepsilon}{2}\|\vec{E}(q)\|^2+\frac{\mu}{2}\|\vec{H}(q)\|^2$$

at the limit $\epsilon\to 0$ it is convenient to consider the Wigner transform [1]. For the six dimensional Faraday vector F^{ϵ} the transform yields a 6×6 matrix density $W^{\epsilon}(q,p)\in \mathrm{Den}(T^*Q)$ on phase space T^*Q defined by

$$W^{\epsilon}_{ij}(q,p)=\frac{1}{(2\,\pi)^3}\int_Q e^{i\,p\cdot r}F_i(q-\frac{\epsilon}{2}r)\,F_j(q+\frac{\epsilon}{2}r)\,dr.$$

The importance of the transform lies in the linear dependence of the electromagnetic energy density $\mathcal{E}(q)$ on the Wigner distribution W^{ϵ},

$$\mathcal{E}(q)=\sum_a\int_{T^*_qQ}\mathrm{tr}(\Pi_a W^{\epsilon})\,dp\,,$$

with Π_a being the projection onto the a^{th} eigenspace of W^{ϵ}, so that on phase space the limit $\epsilon\to 0$ commutes with obtaining the observable from the field variable. With the electromagnetic field being represented by the Wigner transform W^{ϵ}, the dynamics are described by

$$\dot{W}^{\epsilon}=-\{\{W^{\epsilon},p^{\epsilon}\}\}$$

where $\{\{\,,\}\}$ is a matrix-valued Moyal bracket and p^{ϵ} is the symbol of the Maxwell operator P^{ϵ} [1]. In components, the Moyal bracket takes the form

$$\dot{W}^{\epsilon}=\frac{1}{\epsilon}\,(W^{\epsilon}p^{\epsilon}-p^{\epsilon}W^{\epsilon})+\frac{1}{2i}\,(\{W^{\epsilon},p^{\epsilon}\}-\{p^{\epsilon},W^{\epsilon}\})+O(\epsilon).$$

The divergence of the first term $\frac{1}{\epsilon}(W^{\epsilon}p^{\epsilon}-p^{\epsilon}W^{\epsilon})$ at the limit $\epsilon\to 0$ can be evaded by considering transport on the non-trivial eigenspaces π_a of the limit Maxwell symbol p^0 in which case $p^0_a=\tau_a\delta_{ij}$ lies in the ideal of the matrix algebra and multiplication commutes. The eigenvalues of p^0 are [9]

$$\tau_1=0\qquad \tau_2=\frac{c}{n(q)}\|p\|\qquad \tau_3=-\frac{c}{n(q)}\|p\|$$

where c is the speed of light in vacuum and $n(q):Q\to\mathbb{R}$ is the refractive index, and each eigenvalue τ_a has multiplicity two. Considering the projection onto the a^{th} eigenspace, with $\tau_a\neq 0$ on physical grounds, and taking the limit yields [1]

$$\dot{W}^0_a+\{\tau_a,W^0_a\}=[W^0_a,F_a]$$

where $\{\,,\}$ is a matrix-valued Poisson bracket and the eigenvalue λ_a plays the role of the Hamiltonian. W_a^0 in the above equation is the limit of the projection of the Wigner distribution, which in components is given by

$$W_a^0 = \lim_{\epsilon\to 0} (\Pi_a W_a^\epsilon \Pi_a) = \frac{1}{2}\begin{bmatrix} I+Q & U+iV \\ U-iV & I-Q \end{bmatrix} dq\, dp.$$

The parameters I, Q, U, V in W_a^0 are the Stokes parameters for polarization so that $\dot{W}_a^0 + \{\lambda_a, W_a^0\} = [W_a^0, F_a]$ describes the transport of polarized light at the short wavelength limit. For unpolarized light, the regime of classical light transport theory, one has $Q = U = V = 0$ and W_a^0 can be identified with the *phase space light energy density* $\ell = \mathrm{tr}(W_a^0|_{Q=U=V=0}) \in \mathrm{Den}(T^*Q)$. The commutator $[W_a^0, F_a]$, describing the rotation of the polarization during transport, also vansishes in this case, and the time evolution of ℓ is thus described by the *light transport equation*

$$\dot{\ell} = -\{\ell, H\}$$

where we identified the eigenvalue λ_a with the Hamiltonian H, that is $H(q,p) = \lambda_a = \pm\frac{c}{n(q)}\|p\| \in \mathcal{F}(T^*Q)$, with the ambiguity in the sign corresponding to forward and backward propagation in time. The light transport equation emphasizes the Hamiltonian structure of light transport theory, a property that has not been appreciated before (cf. [7]). In our opinion, however, it is of considerable importance because it facilitates the use of a wide range of tools from modern mathematical physics, cf. [8], and provides a necessary first step towards the development of structure preserving computational techniques, cf. [2, 6]. For example, the Hamiltonian formulation shows that geometrical optics can be considered as a special case of light transport theory when the amount of energy that is transported is not considered, and it is also necessary to establish that a five dimensional formulation of the theory on the cosphere bundle $S^*Q = (T^*Q\backslash\{0\})/\mathbb{R}^+$ can be obtained when the symmetry associated with the conservation of the light frequency is considered.

A central result in classical light transport theory is the conservation of radiance along a ray. A modern formulation of radiance, as the energy flux through a two dimensional surface, can be obtained from the light energy density $\ell \in \mathrm{Den}(T^*Q)$ when measurements are considered. What is then still left open, nonetheless, is the symmetry associated with the conservation law, the conservation of the light energy density along trajectories in phase space in our parlance. The associated Lie group action becomes apparent when light transport is considered in idealized environments where the Hamiltonian vector field is defined globally. Time evolution is then described by a curve on the infinite dimensional group $\mathrm{Diff}_{\mathrm{can}}(T^*Q)$ of canonical transformation, establishing that light transport is a Lie-Poisson system with the group $\mathrm{Diff}_{\mathrm{can}}(T^*Q)$ as configuration space and symmetry group [8]. Using the existing theory for such systems [8], light transport can then be reduced from the cotangent bundle $T^*\mathrm{Diff}_{\mathrm{can}}(T^*Q)$ to the dual Lie algebra $\mathfrak{g}^*$, which can be identified with $\mathfrak{g}^* \cong \mathrm{Den}(T^*Q)$, cf. [5]. The infinitesimal coadjoint action in the Eulerian representation $\mathfrak{g}_+^*$, obtained using the right translation action, is equivalent to the light transport equation, $\dot{\ell} = -\mathrm{ad}_H^*\ell = -\{\ell, H\}$, and the convective representation $\mathfrak{g}_-^*$, obtained with the left translation action, is by the change of

variables formula equivalent to the conservation of the light energy density along trajectories in phase space.

A more detailed overview of the geometric structure of light transport theory and its connection to Maxwell's equations is available in [3] and a comprehensive discussion can be found in [4].

References

[1] P. Gérard, P. A. Markowich, N. J. Mauser, and F. Poupaud, *Homogenization limits and Wigner transforms.* Communications on Pure and Applied Mathematics **50** (1997), 323–379.

[2] E. Hairer, C. Lubich, and G. Wanner, *Geometric Numerical Integration.* Springer Series in Computational Mathematics, Springer-Verlag, second ed. 2006.

[3] C. Lessig, A. L. Castro, and E. Fiume, *The Geometry of Radiative Transfer.* arXiv:1206.3301 (June 2012).

[4] C. Lessig, *Modern Foundations of Light Transport Simulation.* Ph.D. thesis, University of Toronto 2012.

[5] J. E. Marsden, A. Weinstein, T. S. and Ratiu, R. Schmid. and R. G. Spencer, *Hamiltonian Systems with Symmetry, Coadjoint Orbits and Plasma Physics.* Atti Acad. Sci. Torino Cl. Sci. Fis. Math. Natur. **117** (1982), 289–340.

[6] J. E. Marsden and M. West, *Discrete Mechanics and Variational Integrators.* Acta Numerica **10** (2001), 357–515.

[7] G. C. Pomraning, *The Equations of Radiation Hydrodynamics.* International Series of Monographs in Natural Philosophy, Pergamon Press 1973.

[8] J. E. Marsden, and T. S. Ratiu, *Introduction to Mechanics and Symmetry: A Basic Exposition of Classical Mechanical Systems.* Texts in Applied Mathematics, Springer-Verlag, third ed. 2004.

[9] L. Ryzhik, G. Papanicolaou, and J. B. Keller, *Transport equations for elastic and other waves in random media.* Wave Motion **24** (1996), 327–370.

Discrete Quasiconformal Mappings of Triangular Meshes

Yaron Lipman

In this talk we present several inroads to open problems in discrete geometry such as the construction of bijective and/or bounded distortion mappings between two dimensional domains and the approximation of polyhedral surfaces' uniformization. The main tool will be the space of quasiconformal piecewise affine mappings. In particular we will study this space of mappings by dissecting it into a collection of convex subspaces.

Simplicial $SL(2,\mathbb{R})$ Chern-Simons theory and Boltzmann entropy on triangulated 3-manifolds

Feng Luo

Given a triangulated oriented 3-manifold or pseudo 3-manifold $(M, \mathcal{T})$, Thurston's equation associated to $\mathcal{T}$ is a system of integer coefficient polynomial equations defined on the triangulation. These polynomial equations are derived from the basic properties of the cross ratio. William Thurston introduced his equation in

the field $\mathbf{C}$ of complex numbers in order to find hyperbolic structures. Due to the important work of Thurston, Neumann-Zagier, Yoshida, Segermann-Tillmann and others, solving Thurston's equation over $\mathbf{R}$ (or $\mathbf{C}$) can be considered as a simplicial $PSL(2,\mathbf{R})$ (or $PSL(2,\mathbf{C})$) Chern-Simons theory since these solutions produce representations of the fundamental group to $PSL(2,\mathbf{R})$ (or $PSL(2,\mathbf{C})$). Our focus is on solving Thurston equation in the field $\mathbf{R}$ of real numbers. Since the classical Chern-Simons theory is variational, it is natural to ask if solutions of Thurston's equation are characterized by a variational principle. The volume optimization program of Casson and Rivin shows that the answer is affirmative for solutions whose values are in the upper-half-plane $\subset \mathbf{C}$. Our main result shows that solutions of Thurston equation over $\mathbf{R}$ are variational with action given by the entropy function.

We achieve this in three steps. In step 1, we introduce a homogeneous Thurston equation on $(M,\mathcal{T})$. This equation is motivated by the vector valued cross ratio. It is shown that solutions of Thurston equation over $\mathbf{R}$ are derived from no-where-zero solutions of the homogeneous Thurston equation. In step 2, using a result of Baseilhac-Benedetti on the existence of $\mathbf{Z}_2$ angle taut structure s, we introduce a closed non-empty convex polytope W_s in $\mathbf{R}^N$ consisting of "angle structures" and define the action functional F on W_s to be the restriction of the entropy function $-\sum_{i=1}^{N} x_i \ln(|x_i|)$. In step 3, we show that the entropy function F is concave in W_s so that the maximum point of F in $int(W_s)$ produces a no-where-zero solution to the homogeneous equation. Furthermore, if the maximum point of F appears in the boundary of W_s, then one can make each tetrahedron in $\mathcal{T}$ an ideal space-like tetrahedron in the anti de Sitter space so that (1) these tetrahedra are glued isometrically along faces producing no shearing at each edge and (2) the signs of dihedral angles of the tetrahedra coincide with the given $\mathbf{Z}_2$ angle taut structure.

This investigation leads to a pentagon relation for the Boltzmann entropy function $f(x) = x\ln(|x|)$. Namely, if $\alpha_1,\alpha_2,\alpha_3,\beta_1,\beta_2,\beta_3$ are real numbers satisfying $\sum_i(\alpha_i+\beta_i)=0$, $\prod_i|\alpha_i| = \prod_i|\beta_i|$ and all but one of them are positive, then

$$\sum_{i,j} f(\alpha_i+\beta_j) = \sum_i (f(\alpha_i)+f(\beta_i)).$$

The geometric meaning of this identity is a mystery to me. The existence of the pentagon relation seems to suggest that there is a topological invariant of 3-manifolds derived from $PSL(2,\mathbf{R})$ Chern-Simons theory. It remains to be seen if there is a quantum version of this identity which should be simpler than the pentagon relation for the quantum dilogarithm.

Uniformization of discrete Riemann surfaces

Stefan Sechelmann
(joint work with Alexander I. Bobenko and Boris Springborn)

On the basis of the notion of discrete conformal equivalence of Euclidean triangle meshes we define discrete conformal equivalence of spherical and hyperbolic triangulations [1, 3, 4]. We consider triangulated surfaces equipped with a metric of constant curvature $K = 0,\ 1,$ or -1 except at the vertices of the triangulation, where the metric is allowed to have cone-like singularities. The discrete metric of such a surface is the function that assignes to each geodesic edge ij its length l_{ij}. Now let $l : E \to \mathbb{R}_{>0}$ be the discrete metric of a triangulated Euclidean surface and let $\tilde{l} : E \to \mathbb{R}_{>0}$ be the discrete metric of an (a) Euclidean, (b) hyperbolic, or (c) spherical surface with combinatorially equivalent triangulation. Then l and $\tilde{l}$ are called *discretely conformally equivalent* if there exists a function $u : V \to \mathbb{R}$ on vertices such that

$$\text{(a) } \tilde{l}_{ij} = e^{\frac{1}{2}(u_i+u_j)} l_{ij}, \quad \text{(b) } 2\sinh\frac{\tilde{l}_{ij}}{2} = e^{\frac{1}{2}(u_i+u_j)} l_{ij}, \quad \text{(c) } 2\sin\frac{\tilde{l}_{ij}}{2} = e^{\frac{1}{2}(u_i+u_j)} l_{ij}.$$

A discrete Riemann surface is an equivalence class of discretely conformally equivalent metrics. It is characterized by the length-cross-ratios defined on edges

$$\mathrm{lcr}_{ij} = \frac{l_{ik} l_{jl}}{l_{kj} l_{li}},$$

where k and l are the vertices of two triangles sharing the edge ij.

The discrete uniformization problem is formulated as follows: Given a discrete metric, find a discretely conformally equivalent Euclidean, spherical, or hyperbolic

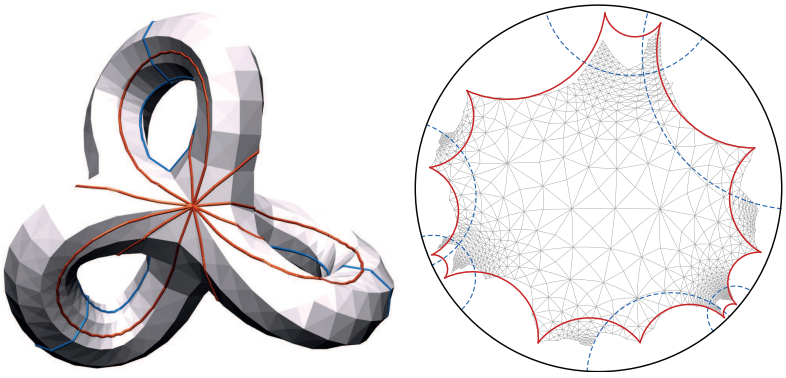

Figure 1. An embedded genus 3 surface and its uniformization. The dashed lines are the axes of the hyperbolic translations that identify corresponding edges of the fundamental polygon. The curves on the embedded surface are the pre-images of the polygon and its axes.

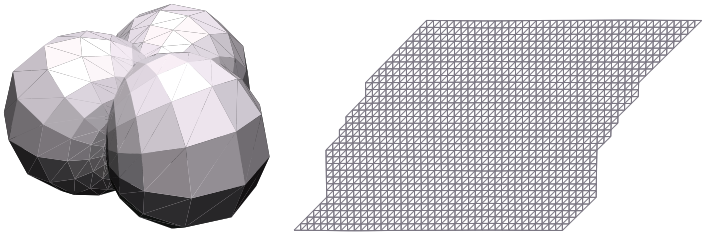

FIGURE 2. Uniformization of a discretely sampled conformal immersion of the Wente torus. The faces of the polyhedral surface are approximate conformal squares. In the discrete uniformization their images are approximately squares, as it should be.

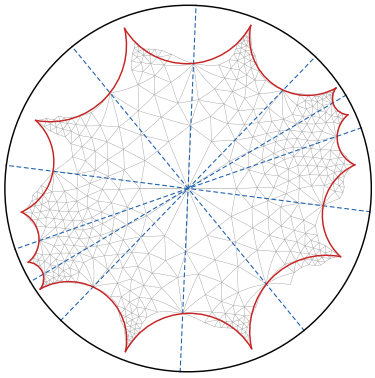

FIGURE 3. Uniformization of a genus 3 hyperelliptic surface created from a two sheeted branched cover of the Riemann sphere. The dashed lines are the axes of the hyperbolic translations that identify opposite sides of the fundamental polygon.

metric without cone-like singularities at vertices, i.e., such that the sum of angles of corresponding triangles around every vertex is 2π. As in the smooth case: For triangulated surfaces of genus $g = 0$, 1, or >1 one obtains a Euclidean, spherical, or hyperbolic discretely conformally equivalent metric, respectively. In all three cases we give a variational description of the corresponding uniformization problem. It is related to volumes of ideal hyperbolic polyhedra [1, 5]. In the Eucliean and hyperbolic case the corresponding functional is convex. Using this technique we show how to calculate standard representations of discrete Riemann surfaces (Figures 1, 2).

For higher genus surfaces we calculate Fuchsian uniformization groups and show different examples for hyperelliptic and general surfaces (Figure 1). We derive a hyperellipticity criterion from the Fuchsian group representation. If and only if the surface is hyperelliptic then in a normalized presentation where opposite sides

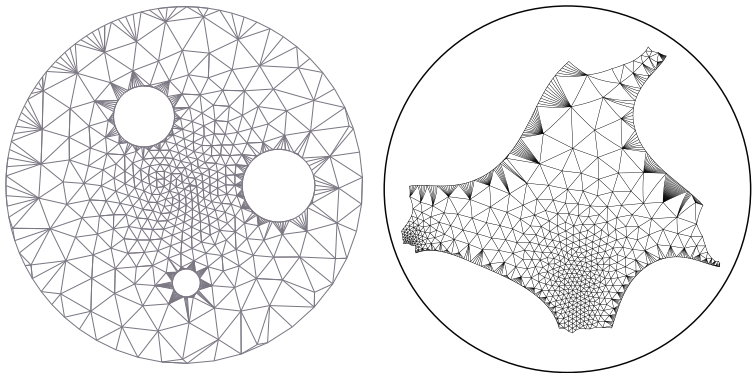

FIGURE 4. Fuchsian uniformization of a discrete Riemann surface given by Schottky data. The fundamental domain is bounded by images of the Schottky-circles and cuts that connect them.

of a fundamental polygon are identified, the axes of the hyperbolic translations meet in a point (Figure 3).

We show how to pass from a Schottky to a Fuchsian uniformization. Here one cannot start with the edge length of a triangulation of a Schottky fundamental domain, since the edges of identified boundaries have different lengths. But the length-cross-ratios $\mathrm{lcr} : E \to \mathbb{R}_{>0}$ are well defined. They determine a discrete conformal class of globally defined discrete metrics l that can be used to obtain a Fuchsian uniformization. The Schottky-circles are mapped to smooth curves in the corresponding Fuchsian uniformization (Figure 4).

References

[1] A. Bobenko, U. Pinkall, B. Springborn, *Discrete conformal maps and ideal hyperbolic polyhedra.* arXiv:1005.2698 (May 2010).

[2] A. I.. Bobenko, S. Sechelmann, B. Springborn, *Uniformization of discrete Riemann surfaces.* In preparation.

[3] F. Luo, *Combinatorial Yamabe flow on surfaces.* Commun. Contemp. Math. **6** (2004), 765–780.

[4] B. Springborn, P. Schröder, U. Pinkall, *Conformal Equivalence of Triangle Meshes.* ACM Transactions on Graphics **27**, Proceedings of ACM SIGGRAPH 2008.

[5] I. Rivin, *Euclidean structures on simplicial surfaces and hyperbolic volume.* Ann. of Math. **139** (1994), 553–580.

Geometric properties of anti-de Sitter simplices and applications

JEAN-MARC SCHLENKER

(joint work with Jeffrey Danciger and Sara Maloni)

Ideal hyperbolic polyhedra have interesting properties that come up in different areas of mathematics. They are uniquely determined by either their dihedral

angles or by their induced metrics, and can also be described by their "shape parameters", which are complex numbers attached to their edges.

We consider ideal polyhedra in the 3-dimensional anti-de Sitter (AdS) space, a Lorentzian space of constant curvature -1 often considered as a Lorentzian analog of hyperbolic space. The complex numbers occuring when considering hyperbolic space are replaced with Lorentz numbers for the anti-de Sitter space. Several statements on ideal hyperbolic polyhedra have analogs for ideal anti-de Sitter polyhedra.

The rigidity properties of those polyhedra are related to those of Euclidean polyhedra with all vertices on a hyperboloid of one sheet.

Convergence of Discrete Elastica

Henrik Schumacher
(joint work with Sebastian Scholtes and Max Wardetzky)

The bending energy of a thin, naturally straight, homogeneous and isotropic elastic rod of length L is given by

$$F(\gamma) = \int_0^L |\kappa(s)|^2 \,\mathrm{d}s,$$

where $\gamma\colon [0,L] \to \mathbb{R}^m$ is the arclength parametrisation and $\kappa = \gamma''(s)$ the curvature vector. Consider the following boundary value problem: Given points P, $Q \in \mathbb{R}^m$ and unit vectors v, $w \in \mathbb{S}^{m-1}$ find the shapes of static elastic curves with clamped ends and fixed length. Defining the space

$$C = \left\{ \gamma \in L^2([0,L];\mathbb{R}^m) \;\middle|\; \begin{array}{c} \gamma' \in L^2([0,L];\mathbb{S}^{m-1}),\ \gamma(0) = P,\ \gamma(L) = Q, \\ \gamma'' \in L^2([0,L];\mathbb{R}^m),\quad \gamma'(0) = v,\ \gamma'(L) = w \end{array} \right\},$$

this can be reformulated to find the minimizers of $F\colon C \to \mathbb{R}$.

A widely used discrete bending energy for a polygonal line $p = (p_0, p_1, \cdots, p_n)$ with $p_i \in \mathbb{R}^m$ is given by

$$F_n(p) = \sum_{i=1}^{n-1} \left(\frac{\varphi_i}{\ell_i}\right)^2 \ell_i,$$

where φ_i is the turning angle and ℓ_i is given by $\ell_i = \frac{1}{2}(|p_{i+1} - p_i| + |p_i - p_{i-1}|)$. We restrict ourselves to evenly segmented polygons, i. e. $|p_i - p_{i-1}| = \frac{L}{n}$ for all $i = 1, \ldots, n$. It is straightforward to formulate a discrete analogon of the boundary value problem above: Find the minimizers of $F_n\colon C_n \to \mathbb{R}$ with the discrete ansatz space

$$C_n = \left\{ (p_0, \ldots, p_n) \in (\mathbb{R}^m)^n \;\middle|\; \begin{array}{c} |p_i - p_{i-1}| = \frac{L}{n},\ p_0 = P,\ p_n = Q, \\ p_1 - p_0 = \frac{L}{n} v,\ p_n - p_{n-1} = \frac{L}{n} w \end{array} \right\}.$$

There has been an attempt by Bruckstein et al. [1] to relate $\operatorname{argmin}(F_n)$ and $\operatorname{argmin}(F)$ via techniques from the theory of epi-convergence. However, epi-convergence of F_n to F only guarantees that *some* minimizers of F can be approximated by those of F_n. We are able to improve this result in various ways:

- The metric on configuration space is strenghtened from Fréchet-distance to $W^{1,2}$-distance.
- We settle some subtleties concerning the length constraint.
- If certain growth conditions of F, F_n can be established, the method yields convergence rates for Hausdorff distance of $\operatorname{argmin}(F)$ and $\operatorname{argmin}(F_n)$.

As metric space we choose

$$X = \left\{\gamma \in W^{1,\infty}([0,L];\mathbb{R}^m) \mid \gamma' \in L^\infty([0,L];\mathbb{S}^{m-1}),\ \gamma(0) = P,\ \gamma(L) = Q\right\}$$

with distance

$$d_X(\gamma_1,\gamma_2) = \left(\int_0^L d_{\mathbb{S}^{m-1}}(\gamma_1'(t),\gamma_2'(t))^2\,\mathrm{d}t\right)^{\frac{1}{2}}, \qquad \gamma_1,\ \gamma_2 \in X.$$

Both C and C_n are contained in X and we extend F, F_n to X by

$$F(\gamma) = \begin{cases} F(\gamma), & \gamma \in C, \\ \infty, & \text{else}, \end{cases} \qquad F_n(\gamma) = \begin{cases} F_n(\gamma), & \gamma \in C_n, \\ \infty, & \text{else}. \end{cases}$$

In general, define

$$\operatorname{argmin}^\delta(F)_\varepsilon = \{x \in X \mid \exists y \in X\colon F(y) \le \inf(F) + \delta \text{ and } d_X(x,y) \le \varepsilon\}.$$

Our main result is

Theorem 2. *For given length and boundary data, there is $c > 0$ s. t.*

$$|\inf(F_n) - \inf(F)| \le \frac{c}{n},$$

$$\operatorname{argmin}(F_n) \subset \operatorname{argmin}^{\frac{c}{n}}(F)_{\frac{c}{n}} \quad \textit{and} \quad \operatorname{argmin}(F) \subset \operatorname{argmin}^{\frac{c}{n}}(F_n)_{\frac{c}{n}}$$

hold.

If F and F_n grow quadratically at their respective minimizers (which appears to be the case generically, but we cannot prove this fact yet), this result implies Hausdorff convergence

$$\operatorname{argmin}(F_n) \overset{n\to\infty}{\longrightarrow} \operatorname{argmin}(F)$$

with convergence rate $\sqrt{\frac{1}{n}}$ in the metric space X.

The proof of Theorem 1 uses techniques which are very much related to the notions of epigraph distances and Attouch-Wets-convergence. (See for example Rockafellar and Wets [2], Chapter 7.) We translate these results to our situation and obtain the following sufficient conditions for Theorem 1 to hold:

- For every global minimizer $\gamma \in C$ of F there is $p \in C_n$ with
$$d_X(p,\gamma) \le \frac{c}{n} \quad \text{and} \quad F_n(p) \le F(\gamma) + \frac{c}{n}.$$
- For every global minimizer $p \in C_n$ of F_n there is $\gamma \in C$ with
$$d_X(\gamma,p) \le \frac{c}{n} \quad \text{and} \quad F(\gamma) \le F_n(p) + \frac{c}{n}.$$

Finally, we show that these conditions are actually fulfilled. Two things are crucial: (i) Minimizers of F have higher regularity than $W^{2,2}$, in particular κ' is bounded. (ii) The energy F and $\|\kappa'\|_{L^\infty}$ of a curve give $\frac{c}{n}$-bounds for the error of suitably chosen polygonal approximations.

References

[1] A. M. Bruckstein, A. N. Netravali and T. J. Richardson, *Epi-convergence of discrete elastica*, Appl. Anal. **79** (2001), 137–171.

[2] R. T. Rockafellar and R. J.-B. Wets, *Variational Analysis*, Grundlehren der mathematischen Wissenschaften, Springer (2004).

Discrete analytic functions: convergence results

Mikhail Skopenkov

This report is on development of discrete complex analysis introduced by R. Isaacs, J. Ferrand, R. Duffin, and C. Mercat [5]. We consider a graph lying in the complex plane and having quadrilateral faces. A function on the vertices is called discrete analytic, if for each face the difference quotients along the two diagonals are equal.

We prove that the Dirichlet boundary value problem for the real part of a discrete analytic function has a unique solution. In the case when each face has orthogonal diagonals we prove that this solution converges to a harmonic function under lattice refinement [6]. This solves a problem of S. Smirnov [7]. This was proved earlier by R. Courant–K. Friedrichs–H. Lewy [4] for square lattices, by D. Chelkak–S. Smirnov [2] and implicitly by P.G. Ciarlet–P.-A. Raviart [3] for rhombic lattices.

We also develop the theory of discrete Riemann surfaces introduced by C. Mercat [5] (the following results are joint with A.I. Bobenko). We prove convergence of discrete period matrices and discrete Abelian integrals to their continuous counterparts [1]. We prove a discrete counterpart of the Riemann–Roch theorem [1].

The methodology is based on energy estimates inspired by direct- and alternating-current networks theory.

The author was supported in part by President of the Russian Federation grant MK-3965.2012.1,"Dynasty" foundation, Simons–IUM fellowship, and grant RFBR-12-01-00748-a.

References

[1] A. I. Bobenko and M. Skopenkov, *Discrete Riemann surfaces: linear theory and its convergence.* Preprint, 2012.

[2] D. Chelkak and S. Smirnov, *Discrete complex analysis on isoradial graphs.* Adv. Math. **228** (2011), 1590–1630, arXiv:0810.2188v2.

[3] P. G. Ciarlet, *The finite element method for elliptic problems.* North-Holland, Amsterdam 1978.

[4] R. Courant, K. Friedrichs, H. Lewy, *Über die partiellen Differenzengleichungen der mathematischen Physik.* Math. Ann. **100** (1928), 32–74. English transl.: IBM Journal (1967), 215–234. Russian transl.: Russ. Math. Surveys **8** (1941), 125–160. `http://www.stanford.edu/class/cme324/classics/courant-friedrichs-lewy.pdf`

[5] C. Mercat, *Discrete Riemann surfaces and the Ising model.* Comm. Math. Phys. **218** (2001), 177–216.
[6] M. Skopenkov, *Boundary value problem for discrete analytic functions.* Submitted (2011), arXiv:1110.6737.
[7] S. Smirnov, *Discrete Complex Analysis and Probability.* Proc. Intern. Cong. Math. Hyderabad, India, 2010, arXiv:1009.6077.

Weighted Averages on Surfaces

Olga Sorkine
(joint work with Daniele Panozzo, Olga Diamanti, Ilya Baran)

We consider the problem of generalizing affine combinations in Euclidean spaces to triangle (PL) meshes: computing weighted averages of points on PL surfaces. Given a triangle PL mesh $\mathcal{S} = (\mathcal{V}, \mathcal{E}, \mathcal{F})$ embedded in $\mathbb{R}^3$, and *anchor points* $\mathbf{p}_1, \mathbf{p}_2, \ldots, \mathbf{p}_N \in \mathcal{S}$ (the anchors can be vertices or anywhere on the mesh's faces). Consider the following function:

$$F(\mathbf{x}) = \sum_{i=1}^{N} w_i \, d(\mathbf{x}, \mathbf{p}_i)^2, \tag{1}$$

where $w_1, \ldots, w_N \geq 0$ are scalar weights such that $\sum_{i=1}^{N} w_i = 1$, and d is a metric on $\mathcal{S}$. If d is the Euclidean metric of $\mathbb{R}^3$ then $F(\mathbf{x})$ has a unique minimum in $\mathbb{R}^3$ which is the regular Euclidean weighted average $\sum_{i=1}^{N} w_i \mathbf{p}_i$. When d is the surface metric and we look for minima of F on $\mathcal{S}$, the result (if it exists and is unique) is called the Fréchet mean.

We are interested in *quickly* solving the *forward* and the *inverse* problems, defined below.

The Forward Problem. We are given scalar weights $w_1, \ldots, w_N \geq 0$ such that $\sum_{i=1}^{N} w_i = 1$. Compute

$$\operatorname*{argmin}_{\mathbf{x} \in \mathcal{S}} F(\mathbf{x}) = \operatorname*{argmin}_{\mathbf{x} \in \mathcal{S}} \sum_{i=1}^{N} w_i \, d(\mathbf{x}, \mathbf{p}_i)^2. \tag{2}$$

The Inverse Problem. Given an additional point $\mathbf{p} \in \mathcal{S}$, compute scalar weights $w_1, \ldots, w_N \geq 0$ such that $\sum_{i=1}^{N} w_i = 1$ and

$$\mathbf{p} = \min_{\mathbf{x} \in \mathcal{S}} \sum_{i=1}^{N} w_i \, d(\mathbf{x}, \mathbf{p}_i)^2. \tag{3}$$

There are clearly many choices of weights for the inverse problem (when d is Euclidean, the inverse problem is generally known as finding (generalized) barycentric coordinates).

Solving the forward problem on a mesh enables applications such as splines on meshes, Laplacian smoothing and remeshing. Combining the forward and inverse problems allows us to define a correspondence mapping between two different meshes based on provided corresponding anchor point pairs, enabling texture transfer, compatible remeshing, morphing and more.

If $\mathcal{S}$ were a C^2 surface and $d(\mathbf{x}, \mathbf{p})$ the geodesic distance between $\mathbf{x}, \mathbf{p}$, then the Fréchet mean is well defined and continuous in w_i and $\mathbf{p}_i$ under some mild conditions (mainly that the distances between anchors are sufficiently small), see [2, 3]. We wish to define the Fréchet mean such that it is reasonably smooth even on PL surfaces. Otherwise splines on meshes will appear jaggy, etc. Moreover, the computation of geodesic distance between arbitrary points on the mesh is computationally expensive, prohibiting real-time interactive applications we have in mind. Hence minimizing $F(\mathbf{x})$ by brute-force search is impractical.

We instead propose to define d by embedding the mesh $\mathcal{S}$ in a higher-dimensional Euclidean space $\mathbb{R}^D$, where Euclidean distances mimic the original geodesic ones. We sample some vertices $\mathbf{s}_1, \ldots, \mathbf{s}_K \in \mathcal{S}$, $K \ll N$, sampling denser in areas of high Gaussian curvature. We then compute the matrix $\mathbf{Q} \in \mathbb{R}^{K \times K}$ of pairwise geodesic distances between all $\mathbf{s}_i$'s:

$$\mathbf{Q}_{i,j} = d_{\text{geo}}(\mathbf{s}_i, \mathbf{s}_j). \tag{4}$$

We then perform the process of so-called Metric Multidimensional Scaling (MMDS), a technique well-established in machine learning. Choosing some D (we use $D = 8$), we solve for positions $\mathbf{e}_1, \ldots, \mathbf{e}_K \in \mathbb{R}^D$ that minimize:

$$\min \sum_{i=1}^{K} \sum_{j=1}^{K} \left(1 - \frac{\|\mathbf{e}_i - \mathbf{e}_j\|}{\mathbf{Q}_{ij}}\right)^2. \tag{5}$$

Now we find the locations $\mathbf{x}_i \in \mathbb{R}^D$ of the rest of the mesh vertices by solving for a biharmonic surface:

$$\Delta^2 \mathbf{x} = 0, \quad s.t.\ \mathbf{x}_i = \mathbf{e}_i \text{ for all sampled vertices.} \tag{6}$$

Here, $\mathbf{x} = [\mathbf{x}_1^T, \ldots, \mathbf{x}_N^T]^T \in \mathbb{R}^{N \times D}$, Δ^2 is the cotangent discretization of the bi-Laplacian [1].

Now that we have our surface embedded in $\mathbb{R}^D$ (including the anchors $\mathbf{p}_i$) and assuming d is the Euclidean metric there, $F(\mathbf{x})$ can be simplified as follows:

$$F(\mathbf{x}) = \sum_{i=1}^{N} w_i \, (\mathbf{x} - \mathbf{p}_i)^T (\mathbf{x} - \mathbf{p}_i) = \sum_{i=1}^{N} w_i \, \mathbf{x}^T \mathbf{x} - 2 \, w_i \, \mathbf{x}^T \mathbf{p}_i + w_i \, \mathbf{p}_i^T \mathbf{p}_i = \tag{7}$$

$$= \|\mathbf{x} - \bar{\mathbf{p}}\|^2 - \bar{\mathbf{p}}^T \bar{\mathbf{p}} + \sum_{i=1}^{N} w_i \, \mathbf{p}_i^T \mathbf{p}_i, \text{ where we denoted } \bar{\mathbf{p}} = \sum_{i=1}^{N} w_i \, \mathbf{p}_i. \tag{8}$$

Note that only the first term, $\|\mathbf{x} - \bar{\mathbf{p}}\|^2$ depends on $\mathbf{x}$, hence minimizing $F(\mathbf{x})$ on $\mathcal{S}$ embedded in $\mathbb{R}^D$ amounts to projecting the regular Euclidean average of the anchor points onto the mesh.

The standard Euclidean projection suffers from the discontinuity problem on the medial axis of $\mathcal{S}$, which is particularly bad for PL surfaces, since there the medial axis touches the surface on every edge. Hence, we are looking for an alternative definition of the projection, which would be continuous and even smooth. Our current idea is to continuously interpolate tangent spaces over the surface. This is not possible to do globally due to "hairy ball" problems, but we consider to perform this locally, such that a consistent projection operator can be defined.

References

[1] Jacobson, A., Tosun, E., Sorkine, O., and Zorin, D., *Mixed finite elements for variational surface modeling.* Comput. Graph. Forum (Proc. SGP) **29** (2010), 1565–1574.

[2] Karcher, H., *Riemannian center of mass and mollifier smoothing.* Communications on pure and applied mathematics **30** (1977), 509–541.

[3] Kendall, W., *Probability, convexity, and harmonic maps with small image i: uniqueness and fine existence.* Proceedings of the London Mathematical Society **61** (1990), 371–406.

Generalized Branching: Making Circles Behave

Ken Stephenson
(joint work with James Ashe and Edward Crane)

Circle packings are configurations of circles with specified patterns of tangency. The geometry that magically emerges in the manipulation of these packings is conformal in nature, as evidenced by the rich theory of discrete analytic functions they have engendered. This discrete theory would be extremely limited, however, if branching were not among its features. It is crucial, for example, in constructing discrete finite Blaschke products, discrete polynomials, and discrete rational functions, just to name a few instances.

The first and most natural notion of branching in circle packing involves a branch circle as the center of a flower whose petal circles wrap multiple times around it [2]. This notion alone allows the theory to advance quite far. In approximating a particular classical polynomial, for example, branching should perhaps be located at specific points, yet there may be no circles centered at those points to carry the branching. In such a situation, placing the branching at nearby circles may harm the detailed properties of the discrete polynomial, but its global character and behavior will be assured — one still obtains a packing which represents a well defined discrete polynomial. This image shows a flower on the left and its branched version on the right; the petals are color coded for identification.

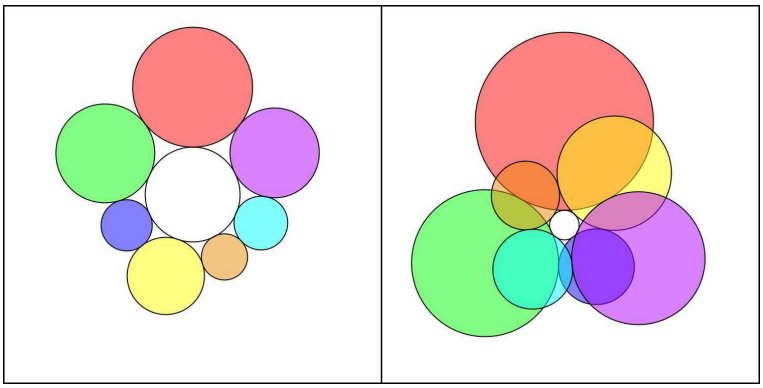

As the discrete theory advances in new directions, however, discretization issues become existential — obstructions must be overcome even to get started with the most basic theory. This talk discusses two key examples: Ahlfors functions on annuli and Weierstrass elliptic functions on tori. With enough symmetry in the combinatorics, all problems may disappear. The next figure illustrates the domain and range of a discrete Ahlfors function; the boundary circles are shaded and the blue circles are symmetrically chosen to be traditional branch circles. The image is a double covering of the unit disc; each of the image circles (other than the branch circles, which are too small to see) represents two circles, one on each sheet.

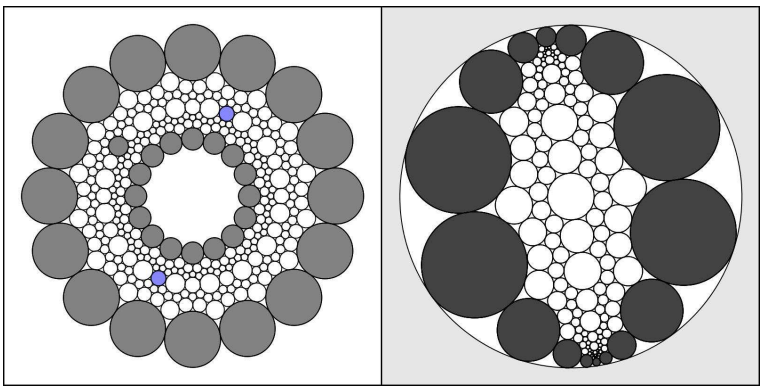

Likewise, the next figure illustrates a discrete Weierstrass function: the domain packing lies on a torus on the left, while the image packing lies on the sphere. There are four branch points and the image is a 2-sheeted covering of the sphere.

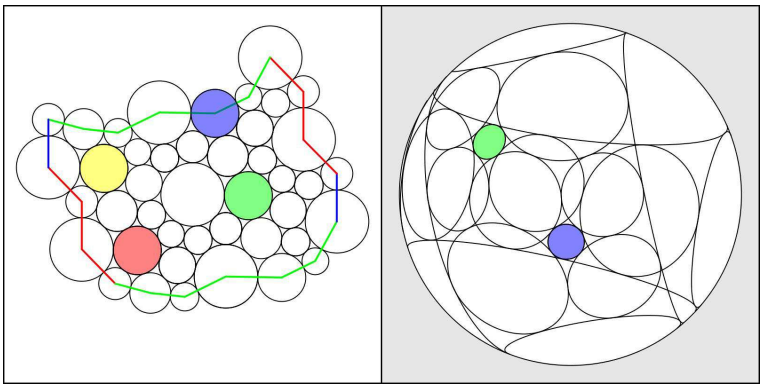

In the absence of combinatorial symmetry, generically there will be no locations for traditional branching that will yield such examples. Hence the need for some new branching paradigm. In this talk we introduce "generalized" branch points into the circle packing machinery [1]. The key idea is to prescribe localized relaxations in packing conditions so that global consistency and integrity can be achieved — give up a little in isolated patches to realize the greater goals. This is quite loose, however, and to gain existence, uniqueness, and convergence results it is necessary to have well delineated (and preferrably minimal) parameterizations of these local relaxations. The following images illustrate two types of generalized branching; in each the unbranched combinatorics are shown on the left, their branched configuration on the right.

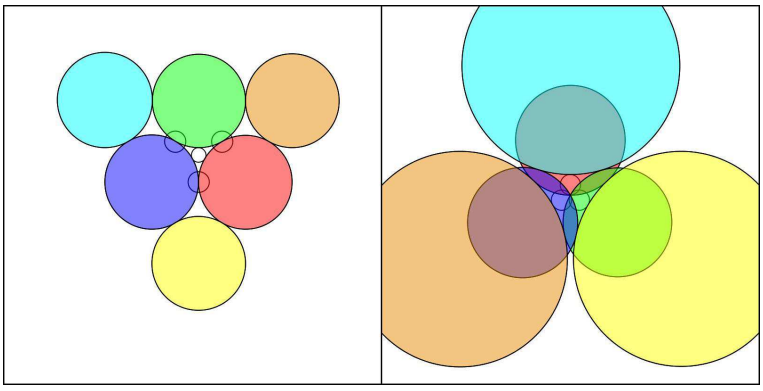

These involve "chaperone" circles and prescribed overlap angles in place of some tangencies. The branching can be difficult to see on the right since, by definition, the circles lie on multiple sheets. These share "local coherence", which means that there is a closed chain of faces around the generalized branch region whose circles will lay out without local holonomy. That outer chain of circles is color coded to match in left and right of each example.

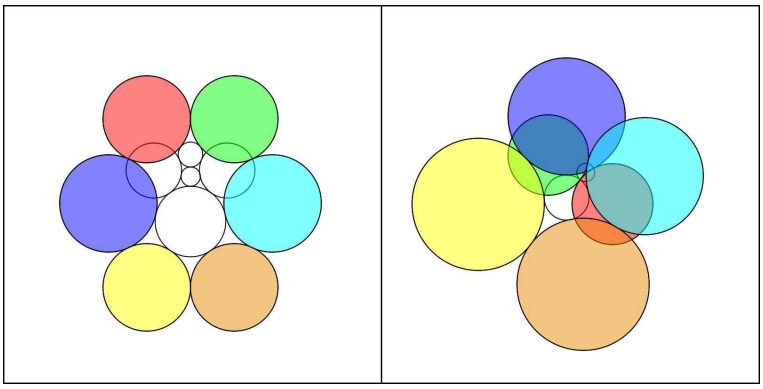

We believe that these two types of generalized branching will allow us the full flexibility available in the classical setting: local coherence ensures they do not introduce local holonomy, yet they can be used to eliminate global holonomy. Of course, having parameters does not mean that finding appropriate branching is easy — in fact it is quite difficult and methods for guaranteeing solutions are under investigation. The talk ends, however, with experiments for an annulus with partial symmetry in its combinatorics; in this instance one can use continuity to find parameters for generalized branching so that the associated discrete Ahlfors function does exist. (The talk was presented as a series of live experiments carried out with the third author's software package *CirclePack* [3].)

References

[1] James Ashe, *Generalized Branching for Coherence in Circle Packing*, PhD Thesis, University of Tennessee, Knoxville, 2012 (advisor: Ken Stephenson).
[2] Kenneth Stephenson, *Introduction to Circle Packing: the Theory of Discrete Analytic Functions*. Camb. Univ. Press, New York, 2005.
[3] Kenneth Stephenson, *CirclePack*, open software available at *http://www.math.utk.edu/∼kens/CirclePack*.

The abstract Hodge–Dirac operator and its stable discretization

Ari Stern
(joint work with Paul Leopardi)

In the numerical analysis of elliptic PDEs, much attention has been given (quite rightly) to the discretization of the second-order Laplace operator. The development of mixed finite elements (e.g., edge elements) paved the way for the discretization of related second-order differential operators, such as the vector Laplacian, with important numerical applications in computational electromagnetics and elasticity. The recent development of *finite element exterior calculus* [1, 2] has shown that these operators are special cases of the *Hodge–Laplace operator* on differential k-forms, which can be stably discretized by certain families of finite element differential forms. An even more general operator, called the *abstract Hodge–Laplace*

operator, includes both the aforementioned Hodge–Laplace operator on k-forms, as well as other operators that arise, for example, in elasticity.

By comparison, *discrete Dirac operators* have received little attention from the perspective of numerical PDEs—despite being, in many ways, just as fundamental as the widely-studied Laplace operators discussed above. Informally, a Dirac operator is a square root of some Laplace operator, and is therefore a *first-order* (rather than second-order) differential operator. Dirac-type operators arise both in analysis [11] and in differential geometry [14], in addition to their well-known, eponymous origins in quantum mechanics [10]. The study of these first-order operators is also associated with a number of celebrated theorems, including the Atiyah–Singer index theorem [3], Witten's proof of the positive energy theorem [17], and the solution of the Kato square root problem [4]. *Clifford analysis* is the study of Dirac operators in various settings, including on smooth manifolds [8, 7].

Recently, there has been growing interest in developing a theory of *discrete Clifford analysis*, based on lattice discretizations of Dirac operators [13, 12, 6]. In many respects, this work resembles the various lattice approaches to discretizing exterior calculus [9, 15, 5], particularly in the use of primal-dual mesh pairs. These approaches are closer in spirit to finite difference methods than to finite element methods, in that they focus more on the degrees of freedom themselves than on basis functions and interpolants. Consequently, these methods tend to be less amenable to stability and convergence analysis, or to higher-order discretizations, compared with finite element exterior calculus. However, scant attention has been given to the possibility of using a mixed finite element approach to discretize Dirac operators and their associated first-order PDEs.

This talk reports on new work [16] which aims to fill this gap. We begin by devloping abstract Dirac operators and Hodge theory in terms of nilpotent operators on Hilbert spaces, following the approach of [4], and introducing a mixed variational problem associated to the Dirac operator. Next, we prove stability estimates, which establish well-posedness for both the continuous and discrete variational problems, as well as convergence estimates, given certain conditions on the discretization. These discretization conditions correspond precisely to similar conditions in finite element exterior calculus, and consequently, we obtain stability and convergence for the well-studied $\mathcal{P}_r$ and $\mathcal{P}_r^-$ finite element families of piecewise-polynomial differential forms. Finally, we show that many of the key estimates in finite element exterior calculus, which apply to discrete Laplace operators, can be recovered as corollaries of our estimates for discrete Dirac operators.

References

[1] D. N. Arnold, R. S. Falk, and R. Winther, *Finite element exterior calculus, homological techniques, and applications.* Acta Numer. **15** (2006), 1–155.

[2] D. N. Arnold, R. S. Falk, and R. Winther, *Finite element exterior calculus: from Hodge theory to numerical stability.* Bull. Amer. Math. Soc. (N.S.) **47** (2010), 281–354.

[3] M. F. Atiyah and I. M. Singer, *The index of elliptic operators on compact manifolds*, Bull. Amer. Math. Soc. **69** (1963), 422–433.

[4] A. Axelsson, S. Keith, and A. McIntosh, *Quadratic estimates and functional calculi of perturbed Dirac operators*, Invent. Math. **163** (2006), 455–497.
[5] P. B. Bochev and J. M. Hyman, *Principles of mimetic discretizations of differential operators.* In: D. N. Arnold et al., Compatible spatial discretizations. IMA Vol. Math. Appl. 142, Springer, New York 2006, 89–119.
[6] F. Brackx, H. De Schepper, F. Sommen, and L. Van de Voorde, *Discrete Clifford analysis: a germ of function theory.* In: I. Sabadini and M. Shapiro and F. Sommen, Hypercomplex analysis. Trends Math., Birkhäuser Verlag, Basel 2009, 37–53.
[7] J. Cnops, *An introduction to Dirac operators on manifolds.* Progress in Mathematical Physics 24, Birkhäuser Boston Inc., Boston, MA, 2002.
[8] R. Delanghe, *Clifford analysis: history and perspective.* Comput. Methods Funct. Theory **1** (2001), 107–153.
[9] M. Desbrun, A. N. Hirani, M. Leok, and J. E. Marsden, *Discrete exterior calculus.* Preprint 2005.
[10] P. A. M. Dirac, *The quantum theory of the electron.* Proc. R. Soc. Lond. A **117** (1928), 610–624.
[11] M. G. Eastwood and J. Ryan, *Aspects of Dirac operators in analysis.* Milan J. Math. **75** (2007), 91–116.
[12] N. Faustino, *Discrete Clifford analysis.* Ph.D. thesis, Universidade de Aveiro 2009.
[13] N. Faustino, U. Kähler, and F. Sommen, *Discrete Dirac operators in Clifford analysis.* Adv. Appl. Clifford Algebr. **17** (2007), 451–467.
[14] T. Friedrich, *Dirac operators in Riemannian geometry.* Graduate Studies in Mathematics 25, AMS, Providence, RI, 2000. Translated from the 1997 german original by Andreas Nestke.
[15] J. Harrison, *Ravello lecture notes on geometric calculus—Part I.* Preprint 2005.
[16] P. Leopardi and A. Stern, *The abstract Hodge–Dirac operator and its stable discretization.* In preparation.
[17] E. Witten, *A new proof of the positive energy theorem.* Comm. Math. Phys. **80** (1981), 381–402.

Lifting Spherical Cone Metrics

John M. Sullivan

Let M^d_κ denote the (simply connected) "model" d-dimensional space of constant curvature κ. (That is, spherical, euclidean, or hyperbolic space, depending on the sign of κ.) A *cone metric* on a (compact) d-dimensional pseudomanifold (with background curvature κ) is obtained by gluing (finitely many) simplices from M^d_κ together along isometries of their facets. Away from the $(d-2)$-skeleton this gives a smooth metric of constant curvature. Around each face of codimension 2 we have some cone angle $\alpha > 0$; the angle defect $2\pi - \alpha$ is a measure of curvature. In particular, the cone metric forms an Alexandrov space of curvature bounded below by κ if and only if all cone angles satisfy $\alpha \le 2\pi$. (Similarly, the metric has curvature bounded above by κ if and only if $\alpha \ge 2\pi$ holds everywhere.)

For $d = 2$, a cone surface has a constant curvature metric away from finitely many cone points. Each cone point contributes an atom $2\pi - \alpha$ of Gauss curvature and the Gauss–Bonnet formula holds in the form $2\pi\chi = \kappa A + \sum(2\pi - \alpha)$, where A is the area of the surface and the sum is over all cone points.

For $d = 3$, the singular locus is an embedded graph with "straight" edges, each with some constant cone angle α. Given an embedded graph in a 3-manifold one can ask which cone metrics exist: for which values of κ and which assigments of

α to each edge is there a corresponding cone metric? The rigidity question asks: when is the cone metric uniquely determined by this data? Even if the metric is not rigid, is the volume – and the length of the singular edges – uniquely determined?

We focus on the case of a link $L = L_1 \cup \cdots \cup L_k$ of k components in $\mathbb{S}^3$. The idea of studying cone metrics basically comes from Thurston, who showed that "most" links are hyperbolic in the sense that for small cone angles α_i around the components L_i there is a hyperbolic ($\kappa = -1$) metric; in the limit $\alpha_i \to 0$ we get a complete hyperbolic metric on $\mathbb{S}^3 \setminus L$. (This metric is unique by Mostow rigidity.)

A standard example, illustrated nicely for instance in the 1991 video *Not Knot* from the Geometry Center, is the Borromean rings, taken with equal cone angles α on all three components. For $\pi < \alpha < 2\pi$ there is a spherical cone metric. (As $\alpha \to 2\pi$ the three singular axes limit to three orthogonally intersecting great circles in the equator of the round 3-sphere. It is known that the Borromean rings cannot be built from three round circles in $\mathbb{S}^3$ but of course we can come arbitrarily close.) For $\alpha = \pi$ we get a euclidean cone metric – the quotient of $\mathbb{E}^3$ by 2-fold rotations around the (non-intersecting, axis-parallel) lines of the primitive cubic rod packing [6]. (Equivalently, the 2-fold cover of $\mathbb{S}^3$ branched over the Borromean rings is a 3-torus admitting a euclidean metric.) For $0 < \alpha < \pi$ we get a hyperbolic cone metric (in particular, for $\alpha = \pi/n$ this corresponds to a hyperbolic metric on an n-fold branched covering), and in the limit $\alpha \to 0$ we get the hyperbolic metric on the link complement.

A *d-orbifold* is a space locally modeled on $\mathbb{R}^d/\Gamma$ for some finite point group Γ. Examples include quotients of M^d_κ by any discrete group of isometries – these inherit "smooth" orbifold metrics, meaning cone metrics with cone angles $\alpha = 2\pi/n$ along the rotation axes of the orbifold.

Thurston used 2-orbifolds as base spaces for Seifert fibrations. These consist of some underlying surface with cone points (those of order n corresponding to $\Gamma = C_n$) and mirror boundaries ($\Gamma = D_1$), which are straight except for coners ($\Gamma = D_n$). To compute the orbifold Euler characteristic χ_o (which is multiplicative even for branched covers) we start with the Euler characteristic of the underlying surface with boundary, and then subtract $1 - 1/n$ for each n-fold cone point (and half that much for each mirror corner).

It is known that every 2-orbifold with $\chi_o < 0$ admits a hyperbolic metric, i.e., is a global quotient of $\mathbb{H}^2$. Similarly there are only 17 orbifolds with $\chi_o = 0$, corresponding to the wallpaper groups and thus having euclidean metrics. For $\chi_o > 0$ we of course have orbifolds corresponding to the finite subgroups of O_3 (the seven polyhedral groups and the seven infinite families of axial groups). But there are also the so-called "bad" orbifolds: spheres with two cone points of orders $1 \le p < q$ (along with their quotients, disks with two corners of orders $1 \le p < q$ on their mirror boundary). These are the base spaces for the (p, q)-Seifert fibrations of $\mathbb{S}^3$ by (p, q)-torus knots, but do not have spherical metrics. (There is no spherical cone metric on $\mathbb{S}^2$ with just two unequal cone points, cf. [5].)

Much of the interest in rigidity of cone metrics in three dimensions has been related to the proofs by Cooper/Hodgson/Kerckhoff and by Boileau/Leeb/Porti

of Thurston's orbifold geometrization conjecture. In an orbifold metric the cone angles satisfy $\alpha \leq \pi$ and many known results are restricted to this range (but see e.g. [2]); we are instead particularly interested in spherical cone metrics with large cone angles.

Given a triangulation of $\mathbb{S}^3$ in which no edge has valence more than 5 – a computer enumeration with Frank Lutz shows there are exactly 4761 such simplicial complexes – we can give each tetrahedron the shape of one from the 600-cell: spherical regular with dihedral angles $2\pi/5$ and edge lengths $\pi/5$. The cone angle around an edge of valence v is then $2\pi v/5$. We get a spherical cone metric of curvature bounded below by 1 in the sense of Alexandrov, leading immediately to diameter and volume bounds. In an ongoing project with Florian Frick, we have focused first on the family whose cone axes (formed by the edges of valence less than 5) are unbranched, forming a link. We have found that most of these are Seifert-fibered, arising as lifts of spherical cone metrics on 2-orbifolds, in the sense we now explain. (The Borromean rings also arise, as do certain graph manifolds.)

Recall that with the exception of hyperbolic and Sol geometries, the remaining six Thurston geometries are those of Seifert fibered spaces, distinguished by the curvature κ of the base and the curvature τ of the bundle [9]. Untwisted bundles ($\tau = 0$) give the geometries $M^2_\kappa \times \mathbb{R}$; twisted bundles ($\tau \neq 0$) give the Berger metrics on $\mathbb{S}^3$ if $\kappa > 0$; Nil or Heisenberg geometry if $\kappa = 0$; and $\widetilde{\mathrm{SL}}(2,\mathbb{R})$ if $\kappa < 0$.

We want to consider such twisted bundles over an aribtrary metric base. That is, we're interested in a Killing submersion from a 3-manifold to a surface, i.e., a submersion where the unit vertical vector field Z is a Killing field, an infinitesimal isometry. The fundamental equations for Riemannian submersions are due to O'Neill [7]. Given a metric disk D with Gauss curvature function κ, and a Killing submersion from $M = D \times \mathbb{R}$, suppose that X and $Y = JX = X \times Z$ are orthonormal horizontal vector fields. Then $\nabla_X Z = \tau Y$ for some function τ on M called the bundle curvature, and we find $\langle [X,Y], Z\rangle = 2\tau$. The sectional curvatures range from $\kappa - 3\tau^2$ for the horizontal plane to τ^2 for any vertical plane, cf. [1].

Suppose we start with a metric on D with $\kappa \geq 1$, then scale down by a factor of two so that $\kappa \geq 4$. Taking $\tau \equiv 1$, the resulting metric on M has all sectional curvatures at least 1. Suppose γ is a closed curve enclosing area A (before rescaling) in the base D. If we lift it to a horizontal curve in M, this lift fails to close and its vertical holonomy is exactly $A/2$ (twice the rescaled area, since $[X,Y] = 2Z + \cdots$). Thus if we want to glue two such metrics together to get a bundle over $\mathbb{S}^2$, we need to take a quotient in the fiber direction, giving circles of some length ℓ. If the total base area is A, then to get the holonomy to match, we need $A/2 = e\ell$ where $e \in \mathbb{Z}$ will be the Euler class of the bundle. That is, to get $\mathbb{S}^3$ with the Hopf fibration we take $e = 1$ and $\ell = A/2$. (For $e > 1$ we get the quotient of this by an e-fold Hopf rotation, giving the lens space $L(e,1)$.)

Consider the case where the base is a spherical cone metric with k cone points of cone angles α_i. Then Gauss–Bonnet says $A = 4\pi - \sum(2\pi - \alpha_i) = 2\pi(2-k) + \sum \alpha_i$. Since the fiber length is $\ell = A/2$ and the projected area is $A/4$ we find the volume of the 3-sphere is $V = A^2/8$. Now consider what happens when we change the α_i.

We obtain $2\,dV = A\,dA/2 = \ell \sum d\alpha_i$, which of course is the well-known Schläfli formula.

There are 17 (not necessarily simplicial) trianguations of $\mathbb{S}^2$ with valence up to 5; giving their triangles the geometry of those in the icosahedron (with area $\pi/5$) we get 17 interesting spherical cone metrics on $\mathbb{S}^2$. Each one Hopf-lifts to give a cone metric on $\mathbb{S}^3$ and indeed these come from triangulations in our family. The lift of an example with f-vector $(k+2, 3k, 2k)$ has vertical length $k\,\pi/5$ and f-vector $\big(k(k+2), k(7k-2), 12k^2, 6k^2\big)$. The lift of the icosahedron is the 600-cell; the lift of the tetrahedron has 8 edges of valence 3 forming a 4-component Hopf link.

Now suppose we are given $1 \leq p < q$ relatively prime and a spherical cone metric on $\mathbb{S}^2$ with one cone point of angle $\beta \leq 2\pi/p$, a second of angle $\gamma \leq 2\pi/q$ and k further ones of angles α_i. We view this as a spherical cone metric on the "bad" pq-orbifold. This we can lift along the (p, q)-Seifert fibration of $\mathbb{S}^3$ to give a cone metric on $\mathbb{S}^3$. Considering the Euler class of the bundle in the orbifold sense [9], we can check that the vertical length must now be $pqA/2$ (where A again is base area). The cone angles are $p\beta$ and $q\gamma$ along the two singular fibers and α_i along a collection of (p, q)-torus knots (i.e., along a (kp, kq)-torus link). This construction accounts for most of the remaining triangulations we have been studying.

Note that in the special case of torus links with equal cone angles along each component, the geometric parameters for these spherical cone metrics have been determined previously via quite different methods [3]; see also [8, 4].

References

[1] J.M. Espinar, I.S. de Oliveira, *Locally convex surfaces immersed in a Killing submersion.* arXiv:1002.1329v1 (2010).

[2] I. Izmestiev, *Examples of infinitesimally flexible 3-dimensional hyperbolic cone-manifolds.* J. Math. Soc. Japan **63** (2011), 581–598.

[3] A.A. Kolpakov, *Addendum to "Spherical structures on torus knots and links"*, preprint (2011), `arXiv:1101.1620v2`.

[4] A.A. Kolpakov, A.D. Mednykh, *Spherical structures on torus knots and links*, Sib. Math. J. **50** (2009), 856–866

[5] F. Luo, G. Tian, *Liouville equation and spherical convex polytopes.* Proc. Amer. Math. Soc. **116** (1992), 1119–1129.

[6] M. O'Keeffe, S. Andersson, *Rod packings and crystal chemistry.* Acta Cryst. A **33** (1977), 914–923.

[7] B. O'Neill, *The fundamental equations of a submersion.* Michigan Math. J. **13** (1966), 459–469.

[8] J. Porti, *Spherical cone structures on 2-bridge knots and links*, Kobe J. Math. **21** (2004), 61–70.

[9] P. Scott, *The geometries of 3-manifolds.* Bull. London Math. Soc. **15** (1983), 401–487.

Spherical geometry and integrable systems

Yuri B. Suris
(joint work with Matteo Petrera)

Nowadays, it is well accepted that geometry provides us with a wealth of important instances of integrable systems. In the present work, it is demonstrated that the cosine law for spherical simplices [7] defines integrable systems in several senses.

For a spherical triangle with the vertices $v_1, v_2, v_3 \in \mathbb{S}^2$, with the sides ℓ_{ij} (connecting v_i and v_j) and the inner angles α_{ij} (opposite to ℓ_{ij}), the cosine law reads as follows:

$$\cos \ell_{ij} = \frac{\cos \alpha_{ij} + \cos \alpha_{ik} \cos \alpha_{jk}}{\sin \alpha_{ik} \sin \alpha_{jk}}. \tag{1}$$

Here (i, j, k) stands for an arbitrary permutation of $(1, 2, 3)$. Putting $x_{ij} = \cos \alpha_{ij}$ and $y_{ij} = \cos \ell_{ij}$, equation (1) is written in the algebraic form:

$$y_{ij} = \frac{x_{ij} + x_{ik}x_{jk}}{\sqrt{1 - x_{ik}^2}\sqrt{1 - x_{jk}^2}}. \tag{2}$$

First interpretation of the spherical cosine law as an integrable system. In this interpretation, the quantities x_{ij} are combinatorially assigned to the three 2-faces of a 3-dimensional cube parallel to the coordinate planes ij, and the quantities $y_{ij} = T_k x_{ij}$ to the three opposite 2-faces, cf. Fig. 1. Here, T_k stands for the unit shift in the k-th coordinate direction. In the terminology of [1], we consider a

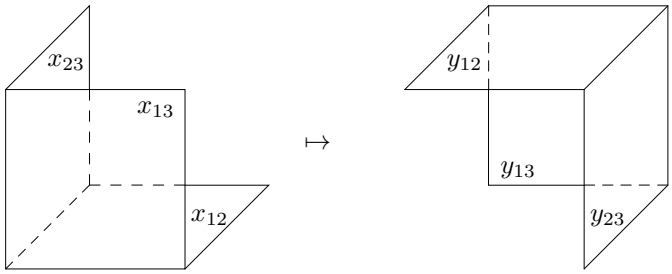

Figure 1. A map on an elementary 3D cube with fields assigned to 2-faces. We interpret y_{ij} as $T_k x_{ij}$, the shift of x_{ij} in the coordinate direction k.

3D system with fields assigned to elementary squares. This 3D system can be called the *symmetric discrete Darboux system*, since it is a special case (symmetric reduction) $x_{ij} = x_{ji}$ of the general *discrete Darboux system*, given by

$$T_k x_{ij} = \frac{x_{ij} + x_{ik}x_{kj}}{\sqrt{1 - x_{ik}x_{ki}}\sqrt{1 - x_{kj}x_{jk}}}. \tag{3}$$

System (3) is well known in the theory of discrete integrable systems of geometric origin. It describes the so called rotation coefficients of discrete conjugate nets

$f : \mathbb{Z}^3 \to \mathbb{RP}^n$, i.e., nets with planar elementary quadrilaterals, see [1, p. 42]. It seems to have appeared for the first time in [4, eq. (7.20)]. Its symmetric reduction $x_{ij} = x_{ji}$ is used for the description of the so called symmetric conjugate nets and discrete Egorov nets, see [2]. The symmetric discrete Darboux system is a close relative of the *discrete CKP system*, see [6]. Thus, symmetric discrete Darboux system admits an novel interpretation in terms of spherical triangles. Recall [1] that integrability of discrete 3D systems is synonymous with their 4D consistency.

Theorem 3. *Symmetric discrete Darboux system is 4D consistent.*

Our new interpretation leads also to a new proof of this (previously known) result. It consists in considering various geometric quantities within a spherical tetrahedron, which combinatorially corresponds to a 4D cube.

Second interpretation of the spherical cosine law as an integrable system. In the second interpretation, we consider the dynamical system generated by (iterations) of map (2) between open subsets of $\mathbb{R}^3$. It can be considered as a time discretization of the famous *Euler top*, described by the following system of differential equations:

$$\dot{x}_{ij} = x_{ik}x_{jk}. \tag{4}$$

The latter system is integrable in the Liouville-Arnold sense, is bi-Hamiltonian and admits integrals of motion $I_i = x_{ij}^2 - x_{ik}^2$, two of which are functionally independent. Discretization (2) of the Euler top turns out to inherit integrability.

Theorem 4. *The map (2) is bi-Hamiltonian and admits integrals of motion*

$$E_i = \frac{1 - x_{ik}^2}{1 - x_{ij}^2}, \tag{5}$$

two of which are functionally independent. It has an invariant volume form

$$\omega = \frac{dx_{12} \wedge dx_{13} \wedge dx_{23}}{\varphi(x)}, \tag{6}$$

where $\varphi(x)$ is any of the functions $(1 - x_{ij}^2)^2$.

Integrals of motion (5) express nothing but the sine law for spherical triangles. An unpleasant non-algebraic nature of discretization (2) is cured in a rather unexpected way.

Theorem 5. *On the subset of $\mathbb{R}^3$ where the second iterate of map (2) is defined, this second iterate is a birational map $x \mapsto \widetilde{x}$ given by the (unique) solutions of the following system of equations:*

$$\widetilde{x}_{ij} - x_{ij} = \widetilde{x}_{ik}x_{jk} + x_{ik}\widetilde{x}_{jk}, \tag{7}$$

which constitute the Hirota-Kimura discretization of the Euler top [3], [5].

Cosine law for spherical tetrahedra as an integrable system. Similarly to the case of spherical triangles, we can consider a dynamical system generated by the map $x \mapsto y$ between open subsets of $\mathbb{R}^6$, where $x_{ij} = \cos\alpha_{ij}$, $y_{ij} = \cos\ell_{ij}$, and α_{ij} and ℓ_{ij} are (opposite) dihedral angles and edges, respectively, of a spherical tetrahedron. This map is given again by the corresponding cosine law. It can be considered as a time discretization of the following system of ordinary differential equations:

$$\dot{x}_{ij} = x_{ik}x_{jk} + x_{im}x_{jm}. \tag{8}$$

Here (i,j,k,m) stands for an arbitrary permutation of $(1,2,3,4)$. This 6-dimensional system turns out to consist of two linearly coupled copies of the Euler top. As a consequence, equations (8) are integrable in the Liouville-Arnold sense, with four independent integrals of motion which can be chosen as

$$x_{12}^2 + x_{34}^2 - x_{13}^2 - x_{24}^2, \qquad x_{13}^2 + x_{24}^2 - x_{23}^2 - x_{14}^2,$$
$$x_{12}x_{34} - x_{13}x_{24}, \qquad x_{13}x_{24} - x_{23}x_{14}.$$

Theorem 6. *The map $x \mapsto y$ defined by the cosine law for spherical tetrahedra admits four independent integrals of motion*

$$\frac{(1-x_{13}^2)(1-x_{24}^2)}{(1-x_{12}^2)(1-x_{34}^2)}, \quad \frac{(1-x_{23}^2)(1-x_{14}^2)}{(1-x_{12}^2)(1-x_{34}^2)}, \tag{9}$$

$$\frac{x_{12}x_{34} - x_{13}x_{24}}{\sqrt{(1-x_{12}^2)(1-x_{34}^2)}}, \quad \frac{x_{13}x_{24} - x_{23}x_{14}}{\sqrt{(1-x_{12}^2)(1-x_{34}^2)}}. \tag{10}$$

It has an invariant volume form

$$\omega = \frac{dx_{12} \wedge dx_{13} \wedge dx_{23} \wedge dx_{14} \wedge dx_{24} \wedge dx_{34}}{\varphi(x)}, \tag{11}$$

where $\varphi(x)$ is any of the functions $(1-x_{ij}^2)^{5/2}(1-x_{km}^2)^{5/2}$.

Again, integrals of motion express nothing but the sine law for spherical tetrahedra.

References

[1] A.I. Bobenko, Yu.B. Suris, *Discrete Differential Geometry. Integrable Structure.* Graduate Studies in Mathematics 98, AMS, 2008.

[2] A. Doliwa, *The C-(symmetric) quadrilateral lattice, its transformations and the algebro-geometric construction*, J. Geom. Phys. **60** (2010), 690–707.

[3] R. Hirota, K. Kimura, *Discretization of the Euler top.* J. Phys. Soc. Japan, **69** (2000), 627-630.

[4] B. G. Konopelchenko, W. K. Schief, *Three-dimensional integrable lattices in Euclidean spaces: conjugacy and orthogonality.* Proc. R. Soc. Lond. A **454** (1998), 3075–3104.

[5] M. Petrera, Yu.B. Suris, *On the Hamiltonian structure of Hirota-Kimura discretization of the Euler top.* Math. Nachr. **283** (2011), 1654-1663.

[6] W. K. Schief, *Lattice Geometry of the Discrete Darboux, KP, BKP and CKP Equations. Menelaus' and Carnot's Theorems.* J. Nonlin. Math. Phys. **10** (2003), 194–208.

[7] E.B. Vinberg (Ed.), *Geometry II.* Encyclopaedia of Mathematical Sciences 29, Springer-Verlag 1993.

Higher pentagram maps, directed weighted networks, and cluster algebras

Serge Tabachnikov

This is a report on a joint work in progress with M. Gekhtman, M. Shapiro and A. Vainstein [3].

Given a convex n-gon P in the projective plane, let $T(P)$ be the convex hull of the intersection points of consecutive shortest diagonals of P. The map T commutes with projective transformations and hence defines a map on the moduli space of projective equivalence classes of polygons. This map was defined by R. Schwartz [13]; it is called the pentagram map. The pentagram map is also defined on a larger class of twisted polygons, that is, polygons with monodromy that is a projective transformation.

The pentagram map has attracted much interest in the recent years; see [14, 15, 9, 10, 16] for a sampler. The main result is that it is a discrete completely integrable system. It was observed by M. Glick [4] that the pentagram map is closely related with the emerging theory of cluster algebras. The goal of our work was to extend the pentagram map to other dimensions and to establish its complete integrability using the techniques of weighted directed networks [11, 2]. Let us mention different approaches to higher dimensional pentagram maps and related systems, developed in [5], in [6, 7], and in [8].

Glick interpreted the pentagram map is a sequence of mutations associated with a special homogeneous bipartite quiver. We generalized Glick's quiver to a family of quivers embedded in the torus. The dual graph of this quiver is a certain weighted directed network on the torus, and the mutations are realized as a sequence of Postnikov moves on this network, followed by a gauge transformations of the respective variables. This results in the family of rational maps T_k:

$$x_i^* = x_{i-r-1}\frac{x_{i+r}+y_{i+r}}{x_{i-r-1}+y_{i-r-1}}, \quad y_i^* = y_{i-r}\frac{x_{i+r+1}+y_{i+r+1}}{x_{i-r}+y_{i-r}}, \quad k \text{ even},$$

$$x_i^* = x_{i-r-2}\frac{x_{i+r}+y_{i+r}}{x_{i-r-2}+y_{i-r-2}}, \quad y_i^* = y_{i-r-1}\frac{x_{i+r+1}+y_{i+r+1}}{x_{i-r-1}+y_{i-r-1}}, \quad k \text{ odd}.$$

where $r = [k/2]-1$, $k \geq 2$. The map T_3 is the pentagram map.

The maps T_k are completely integrable. All the ingredients needed for complete integrability (invariant Poisson bracket, integrals in involution, zero curvature representation) are provided by the "technology" of weighted directed networks, as described in [2]. Specifically, T_k has an invariant Poisson bracket (for $n \geq 2k-1$):

$$\{x_i, x_{i+l}\} = -x_i x_{i+l}, 1 \leq l \leq k-2; \ \{y_i, y_{i+l}\} = -y_i y_{i+l}, 1 \leq l \leq k-1;$$
$$\{y_i, x_{i+l}\} = -y_i x_{i+l}, 1 \leq l \leq k-1; \ \{y_i, x_{i-l}\} = y_i x_{i-l}, 0 \leq l \leq k-2.$$

The functions $\prod x_i$ and $\prod y_i$ are Casimir. If n is even and k is odd, one has four Casimir functions:

$$\prod_{i \text{ even}} x_i, \quad \prod_{i \text{ odd}} x_i, \quad \prod_{i \text{ even}} y_i, \quad \prod_{i \text{ odd}} y_i.$$

The integrals come from the boundary measurement matrix of the respective network. Namely, for $k \geq 3$, let

$$L_i = \begin{pmatrix} 0 & 0 & 0 & \dots & x_i & x_i + y_i \\ \lambda & 0 & 0 & \dots & 0 & 0 \\ 0 & 1 & 0 & \dots & 0 & 0 \\ 0 & 0 & 1 & \dots & 0 & 0 \\ \dots & \dots & \dots & \dots & \dots & \dots \\ 0 & 0 & 0 & \dots & 1 & 1 \end{pmatrix},$$

and for $k = 2$,

$$L_i = \begin{pmatrix} \lambda x_i & x_i + y_i \\ \lambda & 1 \end{pmatrix}.$$

The boundary measurement matrix is $M(\lambda) = L_1 \cdots L_n$. The characteristic polynomial

$$\det(M(\lambda) - z) = \sum I_{ij}(x, y) z^i \lambda^j.$$

is T_k-invariant, and the integrals I_{ij} are in involution.

A geometric interpretation of the maps T_k is as follows.

Let $k \geq 3$, and denote by $P_{k,n}$ the space of projective equivalence classes of generic twisted n-gons in $\mathbf{RP}^{k-1}$. Let $P^0_{k,n} \subset P_{k,n}$ consist of the polygons with the following property: for every i, the vertices V_i, V_{i+1}, V_{i+k-1} and V_{i+k} span a projective plane. These are called corrugated polygons. The consecutive $k-1$-diagonals of a corrugated polygon intersect. The resulting polygon is again corrugated. One gets a pentagram-like $k-1$-diagonal map on $P^0_{k,n}$. For $k = 3$, this is the pentagram map.

Lift the vertices V_i of a corrugated polygon to vectors $\widetilde{V}_i$ in $\mathbf{R}^k$ so that the linear recurrence holds

$$\widetilde{V}_{i+k} = y_{i-1}\widetilde{V}_i + x_i\widetilde{V}_{i+1} + \widetilde{V}_{i+k-1},$$

where x_i and y_i are n-periodic sequences. These are coordinates in $P^0_{k,n}$. In these coordinates, the map is identified with T_k.

The geometric interpretation is different for $k = 2$. Consider the space $\mathbf{S}_n$ of pairs of twisted n-gons (S^-, S) in $\mathbf{RP}^1$ with the same monodromy. Consider the projectively invariant projection ϕ to the (x, y)-space:

$$x_i = \frac{(S_{i+1} - S^-_{i+2})(S^-_i - S^-_{i+1})}{(S^-_i - S_{i+1})(S^-_{i+1} - S^-_{i+2})}$$

$$y_i = \frac{(S^-_{i+1} - S_{i+1})(S^-_{i+2} - S_{i+2})(S^-_i - S^-_{i+1})}{(S^-_{i+1} - S_{i+2})(S^-_i - S_{i+1})(S^-_{i+1} - S^-_{i+2})}.$$

Then x_i, y_i are coordinates in $\mathbf{S}_n/PGL(2, \mathbf{R})$.

Define a transformation $(S^-, S) \mapsto (S, S^+)$, where S^+ is given by the following local "leapfrog" rule: given points $S_{i-1}, S^-_i, S_i, S_{i+1}$, the point S^+_i is obtained by

the reflection of S_i^- in S_i in the projective metric on the segment $[S_{i-1}, S_{i+1}]$. The projection ϕ conjugates this leapfrog map with with T_2. In formulas:

$$\frac{1}{S_i^+ - S_i} + \frac{1}{S_i^- - S_i} = \frac{1}{S_{i+1} - S_i} + \frac{1}{S_{i-1} - S_i},$$

or, equivalently,

$$\frac{(S_i^+ - S_{i+1})(S_i - S_i^-)(S_i - S_{i-1})}{(S_i^+ - S_i)(S_{i+1} - S_i)(S_i^- - S_{i-1})} = -1.$$

Over the field of complex numbers, these formulas can be interpreted as a circle pattern studied by O. Schramm [12]; see also [1].

References

[1] A. Bobenko, T. Hoffmann, *Hexagonal circle patterns and integrable systems: patterns with constant angles.* Duke Math. J. **116** (2003), 525–566.

[2] M. Gekhtman, M. Shapiro, A. Vainshtein, *Cluster algebras and Poisson geometry.* Amer. Math. Soc., Providence, RI, 2010.

[3] M. Gekhtman, M. Shapiro, S. Tabachnikov, A. Vainshtein, *Higher pentagram maps, weighted directed networks, and cluster dynamics.* Electron. Res. Announc. Math. Sci. **19** (2012), 1–17.

[4] M. Glick, *The pentagram map and Y-patterns.* Adv. Math. **227** (2011), 1019–1045.

[5] A. Goncharov, R. Kenyon, *Dimers and cluster integrable systems.* arXiv:1107.5588.

[6] B. Khesin, F. Soloviev, *Integrability of higher pentagram maps.* arXiv:1204.0756.

[7] B. Khesin, F. Soloviev, *The Pentagram map in higher dimensions and KdV flows.* arXiv:1205.3744.

[8] A. Marshakov, *Lie groups, cluster variables and integrable systems.* arXiv:1207.1869.

[9] V. Ovsienko, R. Schwartz, S. Tabachnikov, *The Pentagram map: a discrete integrable system.* Commun. Math. Phys. **299** (2010), 409–446.

[10] V. Ovsienko, R. Schwartz, S. Tabachnikov, *Liouville-Arnold integrability of the pentagram map on closed polygons.* arXiv:1110.0472.

[11] A. Postnikov, *Total positivity, Grassmannians, and networks.* arXiv:math.CO/0609764.

[12] O. Schramm, *Circle patterns with the combinatorics of the square grid.* Duke Math. J. **86** (1997), 347–389.

[13] R. Schwartz, *The pentagram map.* Experiment. Math. **1** (1992), 71–81.

[14] R. Schwartz, *The pentagram map is recurrent.* Experiment. Math. **10** (2001), 519–528.

[15] R. Schwartz, *Discrete monodromy, pentagrams, and the method of condensation.* J. Fixed Point Theory Appl. **3** (2008), 379-409.

[16] F. Soloviev, *Integrability of the Pentagram Map.* arXiv:1106.3950.

Design of Self-supporting Surfaces

Etienne Vouga

(joint work with Mathias Höbinger, Johannes Wallner, Helmut Pottmann)

Vaulted masonry structures are among the simplest and at the same time most elegant solutions for creating curved shapes in building construction. For this reason they have been an object of interest since antiquity, and continue to be an active topic of research today.

We study the combined geometry and statics of *self-supporting* masonry, and develop a tool for the interactive modeling of freeform self-supporting structures.

Here "self-supporting" means that the structure is in static equilibrium under its own weight. This analysis is based on the following classic [8] assumptions: *1)* masonry has no tensile strength, and infinite compressive strength; and *2) (The Safe Theorem)* if a system of forces can be found which is in equilibrium with the load on the structure and which is contained within the masonry envelope then the structure will also carry the loads. A more detailed account of what follows is available in [12].

1. Modeling Self-supporting Surfaces

We model masonry as a surface given by a height field $s(x, y)$ and assume a load density $F(x, y)$ over the top view. The surface is in static equilibrium when there exists a field of symmetric positive-definite matrices $M(x, y)$ satisfying

$$\operatorname{div}(M\nabla s) = F, \quad \operatorname{div} M = 0,$$

where the divergence operator acts on the columns of a matrix [5, 6].

We discretize self-supporting surfaces as a *thrust network* [2]: a mesh $\mathcal{S} = (V, E, F)$ with loads $F_i A_i$ on vertices $\mathbf{v}_i$. Stresses are carried by the edges of the mesh: the force exerted on $\mathbf{v}_i$ by the edge connecting $\mathbf{v}_i, \mathbf{v}_j$ is given by

$$w_{ij}(\mathbf{v}_j - \mathbf{v}_i), \quad \text{where} \quad w_{ij} = w_{ji} \geq 0.$$

The nonnegativity of the individual weights expresses the compressive nature of forces. Equilibrium at vertices is then given by balance of stresses and loads.

Invoking the safe theorem, a masonry structure is self-supporting if we can find a thrust network with compressive forces which is entirely contained within the structure. Finding a self-supporting surface near one that is not amounts to solving for a simultaneous solution in $\mathbf{v}_i$ and w_{ij}. We develop an interactive tool for efficiently finding such a solution: we iteratively alternate between fixing positions and solving for weights w_{ij} that best minimize the least-square error in equilibrium, and fixing the weights and solving for displacements to $\mathbf{v}_i$ that likewise decrease the error. To prevent the surface from drifting too far away from the input shape specified by the user, we regularize the latter step by introducing terms to the objective that penalize total and normal displacement of the vertices.

2. Geometrization of Equilibrium

In both the continuous and discrete settings, static equilibrium of the surface can be formulated in terms of several geometric structures, each with rich connections to discrete differential geometry:

2.1. **Stress Laplacian.** The smooth equilibrium equations can be written in terms of an elliptic Laplace-like operator $\Delta_M = \operatorname{div} M\nabla$. Likewise, the weights w_{ij} define a graph Laplacian Δ_w on the *top view* (projection onto the plane) of the thrust network. This discrete Laplacian is perfect in the sense of [13].

2.2. **Airy Stress Potential.** Symmetry of M together with $\operatorname{div} M = 0$ are integrability conditions on the components of M, so that M is locally determined by the Hessian of a convex real-valued function ϕ (the *Airy stress potential*) [7].

Horizontal equilibrium of the discrete thrust network implies existence of an orthogonal dual to the top view $\mathcal{S}'$, the *reciprocal diagram* [2]. From this dual we construct a convex "Airy stress polyhedron" Φ with planar faces and top view $\mathcal{S}'$ [1]: the gradient jump between two adjacent faces of the stress polyhedron is equal to the edge vector on the reciprocal diagram dual to their shared edge. (If $\mathcal{S}'$ is not simply connected, Φ exists locally.) This Airy stress polyhedron can also be constructed as the finite element discretization of the continuous Airy function [5].

Formulating equilibrium in terms of the Airy stress potential allows us to find PQ remeshings of self-supporting quad meshes where naively introducing a planarity constraint to the optimization fails: the top view of a PQ remeshing must simultaneously admit a PQ remeshing of the stress surface. This can be assured by finding the unique curve networks simultaneously conjugate on ϕ and s [9], given by tracing the eigenvectors of $\nabla^2\phi^{-1}\nabla^2 s$.

2.3. **Isotropic Curvature Relations.** Equilibrium of the surface can be phrased in terms of purely geometric curvature measures of s and ϕ by passing to dual isotropic geometry: $2K_\phi H_s^{\mathrm{rel}} = F$, where K_ϕ is dual-isotropic Gaussian curvature (with respect to the Maxwell paraboloid) and H_s^{rel} is dual-isotropic relative mean curvature. An identical relationship, in terms of mixed-area formulas for discrete curvature [11, 3, 10], holds for discrete thrust networks. As a consequence of this relationship, we can construct special families of self-supporting surfaces, by adding to the dual of a Koenigs mesh [4] a multiple of its Christoffel dual.

References

[1] Ash, P., Bolker, E., Crapo, H., and Whiteley, W., *Convex polyhedra, Dirichlet tessellations, and spider webs.* In: Shaping space (Northampton 1984). Birkhäuser 1988, 231–250.

[2] Block, P., and Ochsendorf, J., *Thrust network analysis: A new methodology for three-dimensional equilibrium.* J. Int. Assoc. Shell and Spatial Structures **48** (2007), 167–173.

[3] Bobenko, A., Pottmann, H., and Wallner, J., *A curvature theory for discrete surfaces based on mesh parallelity.* Math. Annalen **348** (2010), 1–24.

[4] Bobenko, A., and Suris, Yu., *Discrete differential geometry: Integrable Structure.* Graduate Studies in Math. 98, AMS 2008.

[5] Fraternali, F., *A thrust network approach to the equilibrium problem of unreinforced masonry vaults via polyhedral stress functions.* Mechanics Res. Comm. **37** (2010), 198–204.

[6] Giaquinta, M., and Giusti, E., *Researches on the equilibrium of masonry structures.* Archive for Rational Mechanics and Analysis **88** (1985), 359–392.

[7] Green, A., and Zerna, W., *Theoretical Elasticity.* Dover 2002. Reprint of the 1968 edition.

[8] Heyman, J., *The stone skeleton.* Int. J. Solids Structures **2** (1966), 249–279.

[9] Liu, Y., Pottmann, H., Wallner, J., Yang, Y.-L., and Wang, W., *Geometric modeling with conical meshes and developable surfaces.* ACM Trans. Graphics (Proc. SIGGRAPH) **25** (2006), 681–689.

[10] Pottmann, H., and Liu, Y., *Discrete surfaces in isotropic geometry.* In: M. Sabin and J. Winkler (Eds.), Mathematics of Surfaces XII, Springer 2007, 341–363.

[11] Pottmann, H., Liu, Y., Wallner, J., Bobenko, A., and Wang, W., *Geometry of multi-layer freeform structures for architecture.* ACM Trans. Graphics (Proc. SIGGRAPH) **26** (2007), 1–11.

[12] Vouga, E., Höbinger, M., Wallner, J., and Pottmann, H., *Design of self-supporting surfaces.* ACM Trans. Graphics (Proc. SIGGRAPH) **31** (2012).

[13] Wardetzky, M., Mathur, S., Kälberer, F., and Grinspun, E., *Discrete Laplace operators: No free lunch.* In: A. Belyaev and M. Garland (Eds.), Symposium on Geometry Processing. Eurographics Assoc. 2007, 33–37.

Open problems in Discrete Differential Geometry

Collected by Klaus Hildebrandt

Problem 1 (B. Benedetti)**.** Let C be a convex simplicial complex. Is it true that the barycentric subdivision of C is shellable?

So far we can prove a weaker claim: if a complex is convex and d-dimensional, then after at most $d+2$ consecutive barycentric subdivisions it becomes shellable (see my preprint with Karim Adiprasito, `arXiv:1202.6606`).

Glossary: A simplicial complex is called *convex* if it has a geometric realization in some $\mathbb{R}^k$ that is convex. In other words, a convex complex is a linear triangulation of some convex polytope. A triangulated ball B is called *shellable* if its facets can be labeled $1, \ldots, N$, so that the subcomplex determined by the first i facets is a ball (for each $i \leq N$).

History: A connection between shellability and convexity has been known since 1852: The *boundary* of every convex polytope is shellable. (See e.g. Ziegler, Lectures on Polytopes.) In 1958 Mary E. Rudin found an unshellable subdivision of a tetrahedron; so, not every convex complex is shellable. However, the first barycentric subdivision of Rudin's ball is shellable.

Problem 2 (U. Brehm)**.** For a given non-trivial isotopy type of knots (or links) find (approximate numerically) a 2-dimensional branched surface M (standard spine, possibly with 1-dimensional parts) of minimal area having the following property: There exists a knot (or link) $K \subseteq \mathbb{R}^3$ of the given isotopy type such that

(1) $d(M, K) = 1$
(2) M is a deformation retract of $\mathbb{R}^3 \backslash K$.

Exercise: The following should be true and not difficult to show: There exists a pair (M, K) (as specified above) minimizing area(M) and such an M contains an open dense subset consisting of pieces of minimal surfaces and points with distance 1 from K.

Problem 3 (Dmitry Chelkak)**.** Let Γ and Γ^* be two dual planar graphs embedded in the plane so that corresponding dual edges are orthogonal. In this setup, one can naturally introduce discrete ∂ and $\overline{\partial}$ operators acting on functions defined on $\Lambda = \Gamma \cup \Gamma^*$, and the (cotangent-weight) Laplacian $\Delta = 4\partial^*\partial = 4\overline{\partial}^*\overline{\partial}$ which (independently) acts on functions defined on Γ and Γ^*.

Under some mild assumptions on Γ and Γ^* (like "no big faces and no thin angles") prove the following uniform asymptotics of the free Green's function

$$G(u;u_0) = \frac{1}{2\pi}\log|u-u_0| + O(1), \qquad u,u_0 \in \Gamma,$$

and the Cauchy kernel

$$K(v;z_0) = O(|v-z_0|^{-1}), \qquad v \in \Lambda,\ z_0 \in \diamondsuit = \Lambda^*.$$

If Λ is a rhombic lattice (and Γ, Γ^* are isoradial graphs), those asymptotics are known with much higher precision, so the question is how to derive the weaker statement in the more general setup, where no "integrability approach" is available. If proven, the first result would yield most of the "discrete complex analysis toolbox" reported on this workshop, while the second, in particular, would imply the uniform Lipshitzness of discrete harmonic functions (which, as far as we know, remains annoyingly unknown in this case).

Problem 4 (Ivan Izmestiev)**.** Let M be a metrically complete non-compact Euclidean surface with finitely many cone singularities of negative curvature. Is it true that for every point $x \in M$ there exists a geodesic ray starting from x, missing all singular points and escaping to infinity?

MOTIVATION: Joseph O'Rourke posed at the last workshop the problem whether a point in the plane can be shaded by straight segment mirrors. By gluing together two copies of the plane cut along those segments (the left side of each slit to the left, the right to the right), one obtains a Euclidean cone-surface of the kind described above. A light-ray trajectory on the plane is a geodesic on the surface. Thus a positive answer to the question would imply that mirrors cannot shade a point.

Problem 5 (Rick Kenyon)**.** Let T_1, T_2 be two independent and uniformly random triangulations of an n-gon (without internal vertices). Glue these triangulations together along the boundary n-gon to form a triangulation (in the generalized sense) of the 2-sphere. What is the typical or expected diameter of the resulting graph (in the graph metric)? It is conjectured to be of order $n^{1/4+o(1)}$.

Problem 6 (Jürgen Richter-Gebert)**.** This problem comes from characterizing when 10 points in the projective plane lie on a common cubic. In the formulation below it can be considered independent from this geometric interpretation. To formulate the problem we first need a little preparation. We start by considering the following set of ordered triples

$$\begin{aligned} A := \{&(0,1,2),(0,3,4),(0,5,6),(1,3,7),(2,4,7),\\ &(1,5,8),(2,6,8),(3,5,9),(4,6,9),(7,8,9)\} \end{aligned}$$

The combinatorics of these triples comes from the triples of a Desargues configuration. For a permutation $\pi \in S_{10}$ we denote the set of permuted ordered triples by

$$\pi(A) := \{(\pi(i),\pi(j),\pi(k)) \mid (i,j,k) \in A\}$$

and the set of corresponding sets by

$$\overline{\pi(A)} := \{\{\pi(i), \pi(j), \pi(k)\} \mid (i,j,k) \in A\}$$

Since the automorphism group of Desargues configuration has order 120 the set $\{\overline{\pi(A)} \mid \pi \in S_{10}\}$ contains $10!/5! = 30240$ elements. Finally let $X \subset S_{10}$ be a collection of permutations with

$$\{\overline{\pi(A)} \mid \pi \in X\} = \{\overline{\pi(A)} \mid \pi \in S_{10}\}$$

and $|X| = 30240$.

Now we consider 10 points $p_0, \dots, p_9$ in the projective plane presented by homogeneous coordinates. The following is a fact (that is not too difficult to prove): *The points $p_0, \dots, p_9$ are on a common conic if and only if*

$$f := \sum_{\pi \in X} \left(sign(\pi) \cdot \prod_{(i,j,k) \in \pi(A)} \det(p_i, p_j, p_k) \right)$$

vanishes

The expression f is well defined since it turns out that for any two permutations $\pi_1, \pi_2 \in S_{10}$ with $\overline{\pi_1(A)} = \overline{\pi_2(A)}$ we have

$$sign(\pi_1) \cdot \prod_{(i,j,k) \in \pi_1(A)} \det(p_i, p_j, p_k) = sign(\pi_2) \cdot \prod_{(i,j,k) \in \pi_2(A)} \det(p_i, p_j, p_k).$$

QUESTION: Is there a proper subset $X' \subset X$ such that

$$\sum_{\pi \in X'} \left(sign(\pi) \cdot \prod_{(i,j,k) \in \pi(A)} \det(p_i, p_j, p_k) \right)$$

is a factor of f.

Problem 7 (Serge Tabachnikov)**.** An equilateral plane n-gon $V_1V_2 \dots V_n$ is called a bicycle (n,k)-gon if, for all i, the quadrilateral $V_iV_{i+1}V_{i+k}V_{i+k+1}$ is an isosceles trapezoid: V_iV_{i+k+1} is parallel to $V_{i+1}V_{i+k}$ and $|V_iV_{i+k}| = |V_{i+1}V_{i+k+1}|$ (here $2 \le k \le n/2$). In terms of the discrete Darboux transformation [3], a bicycle polygon coincides with its Darboux image, up to a cyclic relabeling. A regular n-gon is a bicycle (n,k)-gon for all k.

The problem is to describe bicycle (n,k)-gons. In particular, for which pairs (n,k) is the regular polygon the only solution to the problem? For example, in the following cases every bicycle (n,k)-gon is regular [4]:
1) n arbitrary and $k = 2$;
2) n odd and $k = 3$;
3) k arbitrary and $n = 2k + 1$;
4) k arbitrary and $n = 3k$.

On the other hand, for k odd and n even, there exists a 1-parameter family of non-congruent bicycle (n,k)-gons. They are constructed by erecting median perpendiculars of the same length to the sides of a regular $n/2$-gon; the resulting

n-gon has dihedral symmetry so, for odd k, its k-diagonals are congruent. One can prove that every bicycle $(4n, n)$-gon is obtained this way.

A regular n-gon is infinitesimally flexible, as a bicycle (n, k)-gon, if and only if

$$\tan\left(kr\frac{\pi}{n}\right)\tan\left(\frac{\pi}{n}\right) = \tan\left(k\frac{\pi}{n}\right)\tan\left(r\frac{\pi}{n}\right)$$

for some $2 \leq r \leq n-2$ ([4]). This equation has the following solutions ([1]): assuming that $r \leq n/2$, one has $k+r = n/2$ and $n|(k-1)(r-1)$. The solutions to this equation that are not covered by the examples from the previous paragraph are second-order flexible but third-order rigid ([2]). Thus one conjectures that these examples are the only examples of bicycle (n, k)-gons with $k < n/2$ (bicycle $(2n, n)$-gons have a considerable flexibility).

The problem has a continuous version that justifies the terminology. The problem is to describe pairs of closed plane curves, the rear and front bicycle tracks, such that one cannot tell which way the bicycle went; a pair of concentric circles provides a trivial example. This problem is equivalent to the 2-dimensional version of Ulam's problem: which uniform bodies float in equilibrium in all positions? See [4] and [5] and the references therein.

References

[1] R. Connelly, B. Csikos, *Classification of first-order flexible regular bicycle polygons.* Studia Sci. Math. Hungar. **46** (2009), 37–46.

[2] B. Csikos, *On the rigidity of regular bicycle (n,k)-gons.* Contrib. Discrete Math. **2** (2007), 93–106.

[3] U. Pinkall, B. Springborn, S. Weißmann, *A new doubly discrete analogue of smoke ring flow and the real time simulation of fluid flow.* J. Phys. A **40** (2007), 12563–12576.

[4] S. Tabachnikov, *Tire track geometry: variations on a theme.* Israel J. Math. **151** (2006), 1–28.

[5] F. Wegner, *Three problems – one solution.* `http://www.tphys.uni-heidelberg.de/~wegner/Fl2mvs/Movies.html`

Reporter: Stefan W. von Deylen

Participants

Karim Adiprasito
Institut für Mathematik I (WE 1)
Freie Universität Berlin
Arnimallee 2
14195 Berlin

Dr. Arseniy Akopyan
Dobrushin Mathematics Laboratory
Institute for Problems of Information Transmission
Bolshoy Karetny per. 19
127994 MOSCOW
RUSSIAN FEDERATION

Prof. Dr. Marc Alexa
Fakultät f. Elektrotechnik u. Informatik
TU Berlin
Einsteinufer 17
10587 Berlin

Dr. Bruno Benedetti
Matematiska Institutionen
Kungl. Tekniska Högskolan
Lindstedtsvägen 25
10044 STOCKHOLM
SWEDEN

Prof. Dr. Alexander I. Bobenko
Institut für Mathematik
Fakultät II - Sekr. MA 8 - 3
Technische Universität Berlin
Straße des 17. Juni 136
10623 Berlin

Prof. Dr. Ulrich Brehm
Institut für Geometrie
TU Dresden
01062 Dresden

Dr. Ulrike Bcking
Institut für Mathematik
Fakultät II - Sekr. MA 8 - 3
Technische Universität Berlin
Straße des 17. Juni 136
10623 Berlin

Cesar Ceballos
Fachbereich Mathematik & Informatik
Freie Universität Berlin
Arnimallee 6
14195 Berlin

Dr. Dmitry Chelkak
St. Petersburg Branch of Steklov Mathematical Institute of
Russian Academy of Science
Fontanka 27
191 023 ST. PETERSBURG
RUSSIAN FEDERATION

Keenan Crane
Department of Computer Science
California Institute of Technology
1200 East California Boulevard
PASADENA CA 91125
UNITED STATES

Prof. Dr. Adam Doliwa
Department of Mathematics and Computer Sciences
University of Warmia & Mazury
ul. Sloneczna 54
10-710 OLSZTYN
POLAND

Andrew Furnas
Department of Mathematics
Brown University
Box 1917
PROVIDENCE, RI 02912
UNITED STATES

Dr. Alexander A. Gaifullin
Dept. of Geometry and Topology
Steklov Mathematical Institute
Gubkina Str. 8
GSP-1 MOSCOW 119991
RUSSIAN FEDERATION

Prof. Dr. Alexander B. Goncharov
Department of Mathematics
Yale University
Box 208 283
NEW HAVEN, CT 06520
UNITED STATES

Felix Gnther
Fachbereich Mathematik
Technische Universität Berlin
Straße des 17. Juni 136
10623 Berlin

Dr. Udo Hertrich-Jeromin
Department of Mathematical Sciences
University of Bath
Claverton Down
BATH BA2 7AY
UNITED KINGDOM

Klaus Hildebrandt
Fachbereich Mathematik & Informatik
Freie Universität Berlin
Arnimallee 6
14195 Berlin

Prof. Dr. Tim Hoffmann
Zentrum Mathematik
TU München
Boltzmannstr. 3
85748 Garching b. München

Dr. Ivan Izmestiev
Fachbereich Mathematik
TU Darmstadt
Schloßgartenstr. 7
64289 Darmstadt

Prof. Dr. Michael Joswig
Fachbereich Mathematik
TU Darmstadt
Dolivostr. 15
64293 Darmstadt

Prof. Dr. Richard Kenyon
Department of Mathematics
Brown University
Box 1917
PROVIDENCE, RI 02912
UNITED STATES

Felix J. Knppel
Institut für Mathematik
MA 8 - 3
Technische Universität Berlin
Straße des 17. Juni 136
10623 Berlin

Dr. Christian Lessig
Department of Computing and
Mathematical Sciences
California Institute of Technology
PASADENA, CA 91125
UNITED STATES

Dr. Yaron Lipman
Department of Computer Science
and Applied Mathematics
The Weizmann Institute of Science
P.O.Box 26
REHOVOT 76100
ISRAEL

Prof. Dr. Feng Luo
Department of Mathematics
Rutgers University
Hill Center, Busch Campus
110 Frelinghuysen Road
PISCATAWAY, NJ 08854-8019
UNITED STATES

Prof. Dr. Christian Mercat
IREM
Universite de Lyon
Batiment Braconnier
43 Bd. du 11 novembre 1918
69622 VILLEURBANNE
FRANCE

Prof. Dr. Ulrich Pinkall
Institut für Mathematik
Technische Universität Berlin
Sekr. MA 3-2
Straße des 17. Juni 136
10623 Berlin

Prof. Dr. Konrad Polthier
Institut für Mathematik
Freie Universität Berlin
Arnimallee 6
14195 Berlin

Prof. Dr. Jrgen Richter-Gebert
Zentrum Mathematik
TU München
Boltzmannstr. 3
85748 Garching b. München

Prof. Dr. Igor Rivin
Department of Mathematics
Temple University
TU 038-16
PHILADELPHIA, PA 19122
UNITED STATES

Dr. Thilo Rrig
Institut für Mathematik
MA 8 - 3
Technische Universität Berlin
Straße des 17. Juni 136
10623 Berlin

Prof. Dr. Raman Sanyal
Institut für Mathematik I
Freie Universität Berlin
Arnimallee 2-6
14195 Berlin

Prof. Dr. Wolfgang K. Schief
School of Mathematics & Statistics
The University of Sydney
SYDNEY NSW 2052
AUSTRALIA

Prof. Dr. Jean-Marc Schlenker
Institut de Mathematiques de Toulouse
Universite Paul Sabatier
118, route de Narbonne
31062 TOULOUSE Cedex 9
FRANCE

Prof. Dr. Peter Schrder
Annenberg Center, CMS
MC 305-16
California Institute of Technology
1200 E. California Blvd.
PASADENA, CA 91125-5000
UNITED STATES

Henrik Schumacher
Institut für Numerische
und Angewandte Mathematik
Universität Göttingen
Lotzestr. 16-18
37083 Göttingen

Stefan Sechelmann
Institut für Mathematik
Fakultät II - Sekr. MA 8 - 3
Technische Universität Berlin
Straße des 17. Juni 136
10623 Berlin

Dr. Mikhail Skopenkov
The Institute for Information
Transmission Problems RAS
Building 1
Bolshoy Karetny per. 19
127994 MOSCOW
RUSSIAN FEDERATION

Prof. Dr. Olga Sorkine
Department of Computer Science
ETH Zürich, CNB G 106.2
Universitätstr. 6
8092 ZÜRICH
SWITZERLAND

Prof. Dr. Boris Springborn
Zentrum Mathematik
Technische Universität München
Boltzmannstr. 3
85747 Garching bei München

Prof. Dr. Kenneth Stephenson
Department of Mathematics
University of Tennessee
320 Ayres Hall
KNOXVILLE, TN 37996-1300
UNITED STATES

Prof. Dr. Ari Stern
Department of Mathematics
Washington University in St. Louis
Campus Box 1146
One Brookings Drive
ST. LOUIS, MO 63130-4899
UNITED STATES

Prof. Dr. John M. Sullivan
Institut für Mathematik
Technische Universität Berlin
Sekr. MA 3-2
Straße des 17. Juni 136
10623 Berlin

Prof. Dr. Yuri B. Suris
Fachbereich Mathematik
Sekr. MA 7-2
Technische Universität Berlin
Straße des 17. Juni 135
10623 Berlin

Prof. Dr. Sergei Tabachnikov
Department of Mathematics
Pennsylvania State University
UNIVERSITY PARK, PA 16802
UNITED STATES

Stefan W. von Deylen
Fachbereich Mathematik & Informatik
Freie Universität Berlin
Arnimallee 6
14195 Berlin

Prof. Dr. Etienne Vouga
Department of Computer Science
Columbia University
NEW YORK NY 10027-7003
UNITED STATES

Prof. Dr. Uli Wagner
Institut de Mathematiques de Geometrie
et Applications
EPFL SB MATHGEOM
MA-C1-533
Station 8
1015 LAUSANNE
SWITZERLAND

Prof. Dr. Johannes Wallner
Institut für Geometrie
TU Graz
Kopernikusgasse 24
8010 GRAZ
AUSTRIA

Prof. Dr. Max Wardetzky
Institut für Numerische
und Angewandte Mathematik
Universität Göttingen
Lotzestr. 16-18
37083 Göttingen

Prof. Dr. Gnter M. Ziegler
Institut für Mathematik
Freie Universität Berlin
Arnimallee 2
14195 Berlin